

INTERRUPTION OF A METABOTROPIC GLUTAMATE RECEPTOR GENE IN
A SMITH-LEMLI-OPITZ SYNDROME PATIENT

BY

TIFFANY LEIGH ALLEY

A DISSERTATION PRESENTED TO THE GRADUATE SCHOOL
OF THE UNIVERSITY OF FLORIDA IN PARTIAL FULFILLMENT
OF THE REQUIREMENTS FOR THE DEGREE OF
DOCTOR OF PHILOSOPHY

UNIVERSITY OF FLORIDA

1997

ACKNOWLEDGMENTS

The last-four-and-a-half years have presented me with the most dramatic changes in my life both academically and personally. I would like to take this opportunity to personally thank all of the individuals who made this journey a bit more tolerable and sometimes downright fun.

I would like to begin by thanking the members of my committee who held on tight while my project took many unexpected turns: Drs. Margaret R. Wallace, Thomas P. Yang, Harry S. Nick, Daniel L. Purich, Charles M. Allen, and Roberto T. Zori. Each member contributed a unique perspective to a very unpredictable project. Their dedication to my graduate success was greatly appreciated.

I am deeply indebted to Dr. Wallace who served in the capacity of a true mentor. She provided an academic environment that nurtured my scientific and personal growth; for this I am grateful. She also showed me that motherhood and career are not mutually exclusive and the only true sacrifice is that of sleep.

Many thanks go to the past and present members of the Wallace laboratory who gave both technical and emotional support: Dr. Steve Colman, Dr. Sonja Rasmussen, Jun Zhang, Jennifer Johnson, Reena Kamath, Sophia Krkljus, Vu Ho, Corinne Abernathy, and Rachael Trimpert. I'd like to extend special thanks to Dr. Steve Colman with whom I developed a friendship that I hope will last a lifetime. Steve was not only my friend, but also my confidant, my emotional punching bag, and sometimes my sanity. I'll never forget the inane bantering or the laughs.

Very few individuals have a lab away from lab, but in this respect I was fortunate. The members of the Nick lab have for years been my surrogate family. I thank them all for the warmth and love they have shown me through the years. Much gratitude goes to my surrogate parents, Dr. Harry Nick and Joan Monnier, for caring about me as if I was their own. And a very special thanks to Dr. Nick for believing in me even when I didn't believe in myself.

Several laboratories directly contributed to my thesis project and deserve to be acknowledged. First, I'd like to acknowledge the laboratory of Drs. Lap-Chee Tsui and Steve Scherer. Their expertise and gracious contributions to my project forged its success. I would also like to thank the members of the R.C. Philips Unit, especially Dr. Roberto Zori and Brian Gray, for their continued technical support.

On a more personal note, I want to thank my family for their unwavering support of my educational pursuits (and my other whims). My family's love for me is only paralleled by my love for them.

Lastly, I would like to acknowledge three individuals who have been essential in my life. Catherine Golden has given me a friendship that knows no boundaries. I appreciated her encouragement and love during my graduate years. I thank Toren Anderson for showing me what love can truly be. He was the driving force behind the completion of my thesis for it enabled us to be reunited. And finally I thank my guardian angel, my mother. It is to her that I dedicate this work, for all her unselfish acts that made this moment possible.

TABLE OF CONTENTS

	<u>page</u>
ACKNOWLEDGMENTS	ii
ABSTRACT	vi
 CHAPTERS	
1 INTRODUCTION	1
Clinical Description of Smith-Lemli-Opitz Syndrome (UF53)	1
Discovery of a Biochemical Defect in Cholesterol Synthesis	6
Case Report of a Severely Affected Smith-Lemli-Opitz Patient	10
Positional Cloning Effort	14
2 IDENTIFICATION OF A YEAST ARTIFICIAL CHROMOSOME SPANNING THE TRANSLOCATION BREAKPOINT IN UF53	17
Introduction	17
Materials and Methods	21
Results	23
Discussion	28
3 IDENTIFICATION OF A METABOTROPIC GLUTAMATE RECEPTOR GENE (GMR8) DIRECTLY DISRUPTED BY UF53'S TRANSLOCATION	30
Introduction	30
Materials and Methods	35
Results	38
Discussion	44
4 PHYSICAL MAPPING OF THE TRANSLOCATION BREAKPOINT REGION	50
Introduction	50
Materials and Methods	56
Results	58
Discussion	59

5	MICROSATELLITE TYPING AND SOUTHERN BLOT ANALYSIS	67
	Introduction	67
	Materials and Methods	72
	Results	74
	Discussion	77
6	CONCLUSIONS AND FUTURE DIRECTIONS	80
	Conclusions	80
	Future directions	83
	REFERENCES	92
	BIOGRAPHICAL SKETCH	105

Abstract of Dissertation Presented to the Graduate School
of the University of Florida in Partial Fulfillment of the
Requirements for the Degree of Doctor of Philosophy

INTERRUPTION OF A METABOTROPIC GLUTAMATE RECEPTOR GENE IN
A SMITH-LEMLI-OPITZ SYNDROME PATIENT

By

Tiffany Leigh Alley

May, 1997

Chairman: Dr. Margaret R. Wallace

Co-Chairman: Dr. Thomas P. Yang

Major Department: Biochemistry and Molecular Biology

Smith-Lemli-Opitz syndrome (SLOS) is an autosomal recessive disorder characterized by facial and limb abnormalities, internal malformations and mental retardation. SLOS patients have an apparent biochemical defect in cholesterol metabolism which results in decreased cholesterol concentrations and a significant increase in 7-dehydrocholesterol (7-DHC), the immediate precursor to cholesterol. The enzyme proposed to be defective in SLOS is 7-DHC reductase (7-DHCR), which converts 7-DHC to cholesterol. The lack of nucleic acid and protein sequence for mammalian 7-DHCR has prevented a definitive link between 7-DHCR and SLOS.

Furthermore, since no *SLOS* gene(s) have been identified, a positional cloning approach was undertaken to identify *SLOS* candidate gene(s). An *SLOS*

patient (UF53) with a de novo balanced translocation in 7q32.1 led to the hypothesis that one *SLOS* allele was interrupted by the translocation while the other allele was inactivated by a more subtle mutation.

Using fluorescence *in situ* hybridization (FISH) with yeast artificial chromosomes (YACs) from a contig of the 7q32 translocation region, one YAC, HSC7E1289, was identified, which spanned UF53's translocation, and other YACs localized proximal and distal to the breakpoint. The contig contains two CpG islands: one is located at the distal end of the contig while the other lies at the distal end of HSC7E1289. A partial cDNA of a metabotropic glutamate receptor (*GRM8*) mapped to the proximal end of HSC7E1289. Southern blot analysis of the mouse homolog of *GRM8* suggested that the *GRM8* gene might be interrupted by UF53's translocation. FISH analysis of cosmids containing *GRM8* exons identified two cosmids, 85b12 and 153a8, which fell directly proximal and distal to the translocation, respectively, implying that *GRM8* was interrupted by the translocation. PCR analysis demonstrated that *GRM8* exon 1 was contained in 153a8 while exon 2 lay in 85b12, indicating that the translocation interrupts *GRM8* in intron 1. This was unexpected since there is no known relationship between *GRM8* and cholesterol biosynthesis. However, *GRM8* is expressed throughout the central and peripheral nervous system during embryogenesis and may play a role in *SLOS* through a mechanism not yet understood.

CHAPTER 1 INTRODUCTION

Clinical Description of Smith-Lemli-Opitz Syndrome

In 1964, Smith, Lemli, and Opitz described a multiple congenital anomalies/mental retardation syndrome in three unrelated males. Originally termed RSH syndrome, representing the initials of each patient, this disorder is better known today as Smith-Lemli-Opitz syndrome or SLOS. SLOS is usually associated with features including (Table 1.1): 1. growth and mental retardation; 2. unusual facies (micrognathia, ptosis, strabismus, anteverted nares, low-set ears, and cleft palate); 3. microcephaly; 4. limb abnormalities (in particular, syndactyly of toes 2-3); 5. pseudohermaphroditism in males; and 6. malformations of the heart, lungs, and gastrointestinal tract (Cherstvoy et al., 1984; Smith et al., 1964). Clinicians also report that photosensitivity and self-abusive behavior are common among SLOS patients (Irons et al., 1995). In addition to clinical manifestations, several studies suggested an underlying metabolic defect including reports of abnormal serum steroids (Chasalow et al., 1985) and low maternal serum estriol levels and sex reversal (McKeever and Young, 1990). Initially it was hypothesized that some SLOS features were due to the direct effect of a genetic mutation(s) on morphogenesis while other anomalies were secondary to the primary defect(s), accounting for the broad spectrum of features (Cherstvoy et al., 1984).

SLOS is inherited as an autosomal recessive trait. This mode of inheritance is supported by reports of recurrence among same sex and different

TABLE 1.1 Manifestations of Smith-Lemli-Opitz Syndrome and UF53 Case Report

Clinical findings	% Frequency in literature	UF53
Developmental		
Birth asphyxia/cyanosis		+
Breech presentation	50	+
Birth weight <2500 g	33	-
Prematurity	25	-
Neonatal feeding difficulties	90	+
Neonatal hypotonia	50	+
Oligohydramnios		-
Prenatal growth deficiency, mild		(50) +
Psychomotor retardation	100	+
Shrill cry		+
Decreased fetal movement		+
Face		
Eyelid ptosis	85	+
Strabismus	40	0 ^a
Cataracts	10	(50) +
Low-set ears	60	+
Broad nasal bridge		-
Anteverted nares	75	+
Cleft posterior palate	40	(60-70) +
Broad maxillary alveolar ridges	60	+
Small tongue		(60) +
Redundant sublingual tissue		-
Micrognathia	80	+
Short neck		+
Cranium/CNS		
Microcephaly	95	(50) +
Narrow high forehead		-
Seizures		-
Ventricular dilation		+
Cerebellar vermis hypoplasia		-
Corpus callosum hypoplasia		+
Limbs		
Postaxial polydactyly	25	(75-85) -
Positional hand abnormalities		+
Short thumbs		+
Transverse/bridged palmar creases	50	+
Fingertip whorls; increased		0
Short proximal limbs		0
Dislocated hips	50	0
Positional foot anomalies		+
Syndactyly, 2-3 toes	65-95	(80) +

TABLE 1.1 continued

Clinical Findings	%Frequency in literature	UF53
Genitalia		
Abnormal/ambiguous in XY males	(100)	N/A ^b
Hypospadias	50	N/A
Bilateral cryptorchidism	50	N/A
Male pseudohermaphroditism	(70)	N/A
Micropenis and/or chordee	20	N/A
Female phenotype in XY males		N/A
Normal genitalia in XX females		+
Gastrointestinal		
Pyloric stenosis	15-25	-
Colon aganglionosis	(35)	+
Gastroesophageal reflux		0
Skin		
Facial hemangioma/ nevus flammeus		+
Loose skin, especially nape of neck		+
Sacral dimple		0
Heart		
Malformations, varied types	20	(50) -
Lungs		
Pulmonary hypoplasia		+
Incomplete lobulation	(57)	0
Renal		
Hypoplastic or solitary		0
Cystic changes, mostly obstructive type		-
Pancreas		
Islet cell hyperplasia	(40-50)	0
Liver		
Hepatic dysfunction		-
Gall bladder anomaly		-
Additional case manifestations		
Loose skin, inner thighs		+
Vertical, tibial skin creases		+

Frequencies were given when available (Wallace et al., 1994).

Parentheses denote frequency in severely affected SLOS patients.

^a information not available.

^b not applicable.

sex sibships with SLOS (Curry et al., 1987; Kohler, 1983; Rutledge et al., 1984) and consanguinity among certain SLOS families (Merrer et al., 1988) in which the parents failed to display the disorder. The incidence of SLOS is between 1:20,000 and 1:40,000 live births (Lowry and Yong, 1980; Opitz, 1994) with an estimated carrier frequency of 1-2% (Chasalow et al., 1985). In unpublished studies of the Swedish population, an SLOS incidence of approximately 1:10,000 was calculated when both live births and miscarriages were taken into account (John Opitz, personal communication). These numbers suggest that SLOS is one of the most common autosomal recessive disorders in the Caucasian population, and its prevalence currently is likely underestimated.

The factor contributing most to the underestimation of frequency is misdiagnosis. Misdiagnosis has been common since the severity can vary dramatically, there is no pathognomonic feature, and several other genetic disorders shares features with SLOS, such as Meckel syndrome (Lowry et al., 1983), Pallister-Hall syndrome (Donnai et al., 1987), and lethal acrodysgenital dwarfism (Merrer et al., 1988). Within the clinical genetics community, the variability in SLOS and its overlap with Meckel syndrome (MS) brought forth the question of whether these two syndromes represented different segments of a broad phenotypic spectrum of a single syndrome. Concordance studies of affected SLOS and MS sibships did not support this theory, though, and several important distinctions between MS and SLOS have since been established, as follows (Lowry et al., 1983). While both MS patients and SLOS patients may display microcephaly, this feature is common in SLOS patients and rare in MS. Although MS patients tend to exhibit encephalocele, they occasionally present with microcephaly in the absence of encephalocele, which is similar to SLOS. Both SLOS and MS males tend to have hypoplasia of external genitalia and cryptorchidism; however, in SLOS males, these features are usually

overshadowed by pseudohermaphroditism. A final feature which led to diagnostic confusion was the presence of orofacial clefts. The distinction, though, was that MS patients typically have cleft lip while SLOS patients have cleft palate. Clearly, accurate diagnosis of SLOS based on clinical features is difficult, leading to misdiagnosis and probable underestimation of the prevalence of SLOS in the general population.

In 1987, Curry et al. proposed classifying a phenotypically distinct category of SLOS as Type II. Common features of SLOS Type II included major structural abnormalities, male pseudohermaphroditism and early lethality. Diagnosis of SLOS Type II was based on the presence of 3 or more of the following: congenital heart defect, postaxial hexadactyly, cataracts, severe genital ambiguity or pseudohermaphroditism in (46, XY) males, cleft palate and small tongue, early death, or the presence of at least one other specific malformation (Johnson et al., 1994). Curry's group felt that Type II represented the extreme end of the SLOS phenotypic spectrum and was far more common than milder SLOS (Type I). SLOS Type II was also believed to be inherited as an autosomal recessive trait. However, it was unclear whether the same gene caused both types. Curry's group reported the existence of intrafamilial concordance of certain features among their cited Type II sibships as well as other previously reported sibships. They reported that affected sibships exhibited either SLOS Type I or Type II with the greatest discordance in longevity. The same year, Opitz and Lowry argued that SLOS Type I and Type II may exist in the same sibship, disputing the concordance so strongly favored by Curry's group (Opitz and Lowry, 1987). The nosology debate over SLOS Type II as a separate entity would not be resolved until 1993, when two collaborative groups discovered a biochemical marker for SLOS shared by both Type I and Type II. Still of debate, though, was whether allelic variation, genetic heterogeneity, or

possibly a contiguous gene syndrome accounted for the broad phenotypic variation seen among SLOS patients.

Discovery of a Biochemical Defect in Cholesterol Synthesis

Several years ago, an apparent biochemical defect in cholesterol biosynthesis was identified in SLOS patients (Irons et al., 1993; Tint et al., 1994). In serum, the defect resulted in a 200- to 2,000-fold increase in the cholesterol precursor 7-dehydrocholesterol (7-DHC) paralleled by a decrease in cholesterol concentrations. This abnormality was also detected in erythrocytes, the lens of the eyes, feces, bile, and cultured fibroblasts from SLOS patients, indicating that the defect was widespread and most likely affected all organs. The enzyme proposed to be defective in SLOS patients was 7-DHC reductase (7-DHCR), which is responsible for the saturation of the C-7 double bond of 7-DHC to produce cholesterol (Tint et al., 1994). The hypothesized 7-DHCR gene seemed an attractive candidate gene for SLOS: however, no nucleic acid or protein sequence is available in mammals (Duvoisin et al., 1995) to establish a definitive correlation between this enzyme and SLOS.

The neutral sterols from the serum and tissues of fasting SLOS patients were identified and their levels measured by capillary-column gas chromatography (Tint et al., 1994). Several abnormal sterols were detected in the serum and tissues of all SLOS patients studied. The most prominent sterol was identified as 7-DHC and represented the largest sterol fraction in these patients. The two other sterols were later identified as 8-dehydrocholesterol (8-DHC), an isomer of 7-DHC, and 19-nor-5,7,9(10)-cholestatrien-3 β -ol (Batta et al., 1995). Although 8-DHC is not a precursor to cholesterol, it is believed to be formed from 7-DHC by an unidentified isomerase found in the hepatic microsomes. The abnormal sterol 19-nor-5,7,9(10)-cholestatrien-3 β -ol is seen in some but not all

affected individuals; its origin is still unknown. Although no correlation between the severity of SLOS and the levels of 7-DHC and 8-DHC has yet been established, these sterols appear to be significantly more elevated in severely affected patients. Conversely, 19-nor-5,7,9(10)-cholestatrien-3 β -ol seems to be in similar quantities in both mildly and severely affected patients, about 10% of total sterols, when present. It should be noted that the total sterol content does not appear to be abnormally low since the elevated 7-DHC and presence of aberrant sterols compensate for the cholesterol deficiency.

In cholesterol biosynthesis, the pathway becomes branched after the formation of lanosterol (Figure 1.1) in which either the side chain C-24 double bond is saturated immediately or as the final step (Clayton, 1965). In the case of early C-24 saturation, the following cholesterol precursors include 24,25-dihydrolanosterol, lathosterol, and 7-DHC. The other branch of the pathway proceeds through a series of intermediates with an unsaturated side chain, C-24, including cholest-5,7,24-triene-3 β -ol and desmosterol. It is generally accepted that these two pathways do not constitute separate and mutually exclusive pathways, but instead share certain enzymes including 7-DHC reductase and 3 β -hydrosterol Δ^{24} -reductase, the enzyme responsible for reducing the C-24 double bond (Steinberg and Avigan, 1960).

In higher eukaryotes, cholesterol constitutes up to one-third of the lipid membrane and is an essential component of the cell membrane and outer mitochondrial membrane (Opitz et al., 1994). Cholesterol and its intermediates are not only responsible for maintaining membrane integrity, but is also involved in production of steroid hormones, bile acids, and vitamin D; protein glycosylation, and myelination of the central and peripheral nervous system (Acosta, 1995). In addition, *de novo* cholesterol synthesis is intricately involved in the development of the testis, liver and brain (Ness, 1994). Considering the

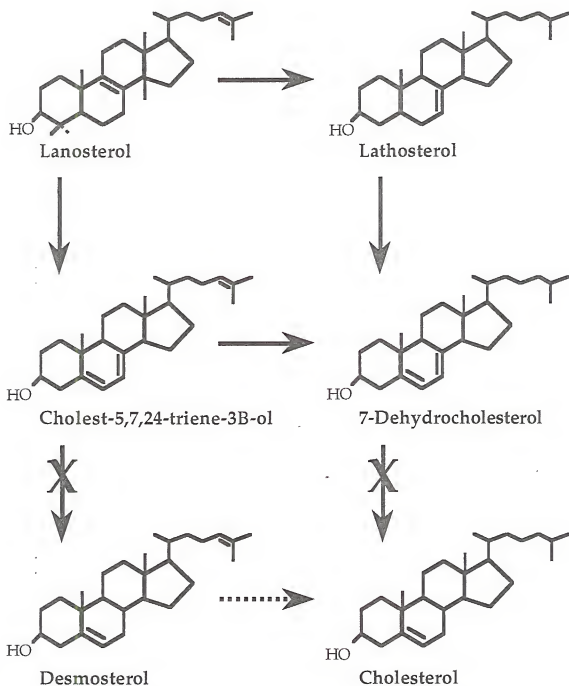


Figure 1.1. Schematic representation of cholesterol biosynthesis from lanosterol (Tint et al., 1995). The right side of the pathway demonstrates early saturation of the C-24 bond (7-DHC conversion to cholesterol is penultimate step) while the left side demonstrates late saturation. In SLOS, it is proposed that both branches have a block in cholesterol biosynthesis, indicated by the Xs, at the level of saturation of the C-7 double bond by 7-DHCR.

ubiquitous nature of cholesterol, it seems plausible that a defect in its biosynthesis could be the underlying mechanism for the widespread damage seen in SLOS. However, the proposition of 7-DHCR as an SLOS candidate gene is based strictly on circumstantial evidence since its involvement in SLOS at a molecular level has not been corroborated experimentally.

Analysis of the urinary bile acids of SLOS patients by continuous flow fast atom bombardment mass spectrometry uncovered two abnormalities (Natowicz and Evans, 1994). First, normal urinary bile acids (cholanoates) were absent or at subnormal concentrations. Cholanoates are essential in emulsification and absorption of dietary fats (Acosta, 1995). This deficiency could thus account for the feeding difficulties seen in 90% of SLOS patients. Second, the bile acids that were present were abnormal: there was an added unit of unsaturation, suggesting that 7-DHC may be further processed into bile acids in the presence of the defect in cholesterol biosynthesis.

Cholesterol synthesis begins in the fetal adrenal glands and liver at about 8 and 10 weeks, respectively (Acosta, 1995). The accumulation of 7-DHC in SLOS fetuses would presumably begin with the initiation of cholesterol synthesis during the first trimester. The effects of 7-DHC accumulation on development, cholesterol biosynthesis regulation, placental transfer of cholesterol, cell membrane transport, and membrane permeability at this developmental stage are still unknown.

Although the molecular basis connecting the defect in cholesterol biosynthesis and SLOS has yet to be proven, both diagnosis and prenatal testing for SLOS are now possible based on examination of the cholesterol and total sterol profile. Prior to the biochemical discovery, women at risk for carrying an SLOS fetus could obtain prenatal diagnosis based only on detection of a gross anatomical defect, using by transvaginal ultrasonography during the first

trimester (Hobbins et al., 1994). Unfortunately, ultrasonography may fail to detect milder cases of SLOS. Today, prenatal diagnosis is based on the measurement of 7-DHC in amniotic fluid and chorionic villi sampling (Dallaire et al., 1995; Mills et al., 1996). This method allows for detection of the abnormal cholesterol profile in a fetus as early as the first trimester.

Several other disorders display a defect in cholesterol biosynthesis reflected by a deficit in serum cholesterol concentrations, such as hypobetalipoproteinemia (Linton et al., 1993). SLOS, though, is unique in that patients not only have low levels of circulating cholesterol but also show low levels in all tissues studied, indicating a disturbance of the endogenous production of cholesterol. However, it can not be ruled out that this metabolic defect is secondary to a primary defect (other than in 7-DHCR) not yet elucidated. Characterization of the molecular defect(s) in SLOS is thus crucial for further understanding of this disorder, as well as to improve diagnosis.

Case Report of a Severely Affected SLOS Patient, UF53

In 1994, our group reported an affected Caucasian female (UF53) displaying the severe phenotype of SLOS (Wallace et al., 1994). The patient presented with the characteristic SLOS facies (micrognathia, cleft palate, ptosis, anteverted nares, hypoplastic tongue), developmental delays, syndactyly of toes 2-3, limb abnormalities, Hirschsprung disease and microcephaly (refer to Table 1.1 and Figure 1.2). UF53 was the only affected sib of three children born to normal parents with an unremarkable family history. Prior to the child's death at 5-months of age, lymphoblastoid and skin fibroblast cultures were established, and DNA was obtained from the parents' leukocytes. No autopsy was performed.

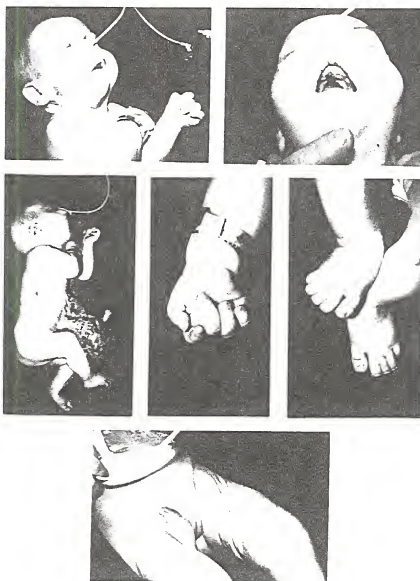


Figure 1.2. Photographs of UF53 displaying the severe form of SLOS (Wallace et al., 1994). The unusual facies (ptosis, strabismus, micrognathia, cleft palate, and broad nasal bridge) and microcephaly associated with SLOS are shown in the top panels. Note also the colostomy bag resulting from surgery for Hirschsprung disease and the 2-3 toe syndactyly, both commonly seen in the severe form of the disease.

The defect in cholesterol biosynthesis had yet to be discovered at the time of UF53's diagnosis, therefore biochemical testing of the patient's serum neutral sterol concentrations was not possible. It was observed though, that at age 3 weeks and 5 weeks, the patient had serum cholesterol levels of 45 and 55 mg/dL, respectively. This is in contrast to the serum cholesterol levels of normal 3-month-old children fed low cholesterol corn-soybean oil-based diets, which are reported to be 109 ± 9 mg/dL (Hayes et al., 1992). I later confirmed the defect in cholesterol metabolism in UF53 by analysis of the fibroblast cultures, in collaboration with Dr. Steve Tint (Alley et al., 1995). To confirm the clinical diagnosis of SLOS in UF53, fibroblast cultures grown in delipidated medium (cholesterol-deficient) were sent to Dr. Tint (Veteran's Hospital, East Orange City, New Jersey) for analysis of cholesterol and 7-DHC levels. His studies detected the SLOS abnormal sterol profile in UF53. Normal fibroblasts have cholesterol concentrations of 40-60 mg/ 2×10^6 cells with a complete absence of 7-DHC. Cholesterol and 7-DHC concentrations in UF53 fibroblasts were 19 and 2.7 mg/ 2×10^6 cells, respectively. The results of the assay clearly demonstrated that UF53 had a dramatic decrease in cholesterol concentration while 7-DHC was significantly elevated. Together, the clinical presentation and the presence of the aberrant cholesterol profile confirmed the diagnosis of SLOS.

Of particular interest in UF53, though, was the presence of a *de novo* balanced translocation between the long arms of chromosomes 7 and 20, [t(7;20)(q32.1;q13.2)], detected by routine cytogenetic studies (Wallace et al., 1994). The idiogram in Figure 1.3 schematically represents the breakpoint assignments to 7q32.1 and 20q13.2, which were made at a resolution of 650-800 bands/haploid set of chromosomes. The *de novo* appearance of both the translocation and SLOS in UF53 suggested a possible etiological connection. Therefore, based on this hypothesized connection, UF53's translocation served as

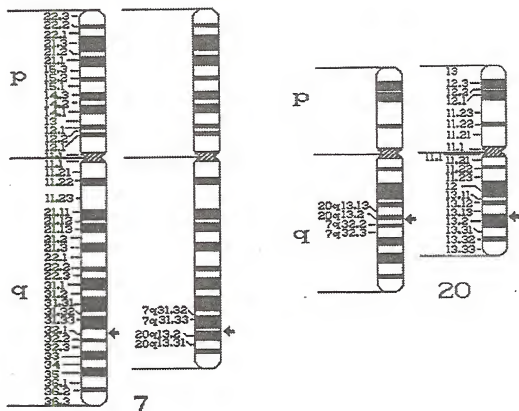


Figure 1.3. Schematic representation of the karyotype, $[t(7;20)(q32.1;q13.2)]$, resulting from UF53's translocation between the long arms of chromosome 7 and chromosome 20 at q32.1 and q13.2 (indicated by the arrows), respectively (Wallace et al., 1994).

a physical landmark for positional cloning efforts in the elucidation of the causative *SLOS* gene.

Positional Cloning Effort

Positional cloning is a method of isolating disease-causing genes based on the relative chromosomal location of the gene rather than knowledge of the etiological basis of the disorder (functional cloning). Although *SLOS* has an apparent biochemical defect in cholesterol biosynthesis, the lack of 7-DHCR protein sequence eliminates the possibility of functional cloning based on this proposed defect.

Figure 1.4 illustrates the general approach to positional cloning. Most positional cloning efforts begin with the genetic linkage of a disorder to a broad chromosomal location based on its segregation in families with polymorphic markers. In the case of *SLOS*, linkage was not a feasible approach for several reasons: 1. lack of large families; 2. diagnostic difficulty in adults, as abnormal features lessen with age (de Die Smulders and Fryns, 1992); and 3. the possibility of genetic heterogeneity, which could prevent linkage detection. Hence, the discovery of UF53's translocation was fortuitous since gross chromosomal rearrangements act as physical landmarks for positional cloning of disease genes when linkage is not available. UF53's translocation offered a unique resource in the search for a putative *SLOS* gene due to the *de novo* appearance of the chromosomal rearrangement and *SLOS* in this patient. Several human disease genes have been cloned based on the presence of translocations including neurofibromatosis type 1 (Wallace et al., 1990), Duchenne muscular dystrophy (Monaco et al., 1986), choroideremia (Cremers et al., 1990), and adult polycystic kidney disease (Wunderle et al., 1994).

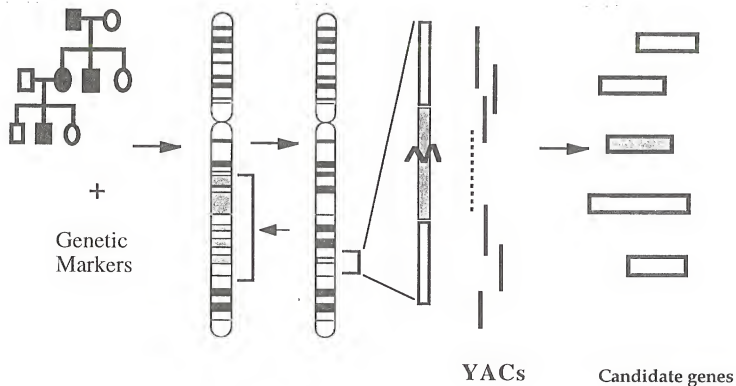


Figure 1.4. Schematic of the general approach to positional cloning. Initially, family pedigrees are collected in which the disease gene is segregating. These families are studied with various markers until there is evidence which links on or more of the markers to the disease. The region is further narrowed by additional linkage. The existence of a translocation allows for the quick advancement to the cytogenetic level. In order to narrow the region of interest, one would try to identify large genomic clones, such as YACs in the region. Once the region of interest has been narrowed to the kilobase level, various methods can be employed to identify candidate genes in the region.

I chose to begin positional cloning efforts at the 7q32.1 region, rather than chromosome 20, based on literature review which suggested that an *SLOS* locus resided in the distal 7q region. This assignment was based on several reports of individuals with SLOS and SLOS-like features with chromosomal deletions in the 7q32-qter region (Berry et al., 1989; Bogart et al., 1990; Schwartz et al., 1983; Young et al., 1984). More convincing, though, was the report of another severely affected SLOS male with a maternally inherited balanced translocation involving 7q32 (Curry et al., 1987). To fit the autosomal recessive model, I hypothesized that UF53's translocation disrupts a putative *SLOS* allele, at 7q32.1, while a more subtle, inherited, mutation disrupts the other allele.

CHAPTER 2 IDENTIFICATION OF A YEAST ARTIFICIAL CHROMOSOME SPANNING UF53'S TRANSLOCATION

Introduction

In positional cloning, once a chromosomal location has been established, a variety of methods can be employed to successively narrow the region of interest. To more finely map UF53's translocation from a cytogenetic level to a kilobase (kb) level, I intended to pursue two methods: somatic cell hybridization and fluorescence *in situ* hybridization (FISH). Both methods have been extensively used in the elucidation of the human genomic map and would directly establish position of large clones, such as yeast artificial chromosomes (YACs) and cosmids, relative to rearrangements such as the UF53 translocation (Brock, 1993; Rothwell, 1993).

Somatic cell hybridization is a method in which somatic cells from two different species, usually human and rodent, are fused together in the presence of polyethylene glycol or Sendai virus. These agents alter the cell membranes in such a way that fusion is enhanced and cells from the different species form a single cell with two nuclei called a heterokaryon. These heterokaryons are then grown in HAT medium which selects for hybrids containing nuclei from both species, due to complementation of a mutation in the rodent cells. The selected, newly-formed cells have a tendency to lose the human chromosomes while maintaining the rodent background. Since this loss is random, each clone differs

in its human chromosome complement. After the initial loss of chromosomes, stable cell lines from the clones can be established since no additional chromosome loss rarely occurs.

The goal was to establish individual somatic cell hybrids from UF53's cell lines: one containing the derivative 7 chromosome, one having the derivative 20 chromosome, and one having the normal 7 chromosome. With these hybrids, the location of genomic clones and cDNAs relative to the translocation could be established based on sequence complementation to this region using Southern methodology. Fibroblast cell lines were sent to Dr. James P. Evans (University of Washington, Seattle) to establish somatic cell hybrids, but unfortunately all attempts at fusion failed. A second attempt was made by Dr. David Cox (Stanford University, California) to produce hybrids using both the fibroblast and lymphoblastoid cell lines from UF53. Repeated experiments using both cell lines against several rodent backgrounds also resulted in failure. It was suggested that the inability to establish somatic cell hybrids was possibly due to the abnormal sterol composition in the cell membranes in UF53, the result of the cholesterol biosynthesis defect or some other abnormality specific to UF53 or SLOS (Dr. David Cox, personal communication). Further attempts to establish somatic cell hybrids were abandoned.

As an alternative, FISH was developed to localize large genomic clones, such as yeast artificial chromosomes (YACs) and cosmids, relative to the UF53 translocation. Chromosome *in situ* hybridization is based on the concept that a labeled genomic clone (probe), when heated, will denature into single-stranded forms that will anneal to complementary sequence on a denatured chromosome, producing a hybridization signal which reveals the probe's cytogenetic location (Figure 2.1). Figure 2.2 represents the three possible outcomes (distal, proximal, or spanning) resulting from the hybridization of a YAC clone against UF53's

FISH

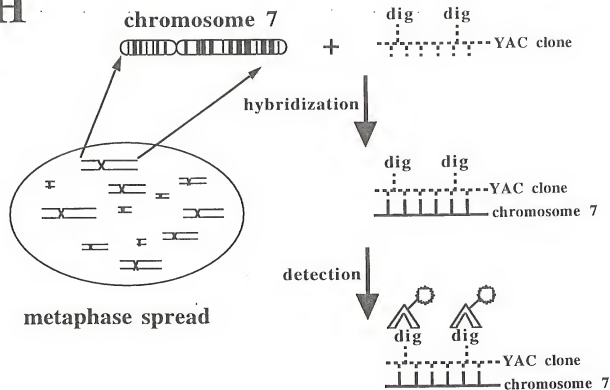


Figure 2.1. Illustration of FISH analysis. The patient's metaphase chromosomes, shown in the circle, are denatured and hybridized with a biotin- or digoxigenin-labeled genomic clone (i.e. YAC clone). The YAC clone anneals to its homologous sequence on the chromosome (i.e. chromosome 7). The hybridization is detected by using fluorescently-tagged antibodies specific to biotin or digoxigenin and then detected by fluorescent microscopy.

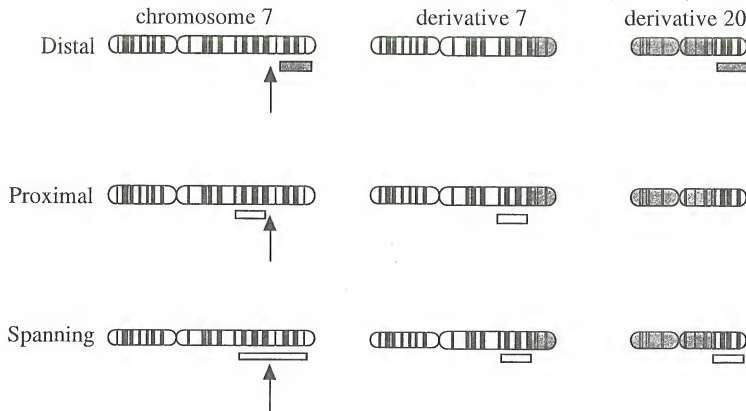


Figure 2.2. Schematic representation of expected FISH results. A genomic clone which hybridizes distal (shown as a blue box) or proximal (shown as a yellow box) to the breakpoint will have a hybridization signal on the normal chromosome 7 and on the derivative chromosome 20 or derivative chromosome 7, respectively. A genomic clone spanning the translocation (shown as a green box) will have hybridization signals on the normal chromosome 7 and both derivative chromosomes.

metaphase spreads. One of three outcomes was expected from each FISH experiment. In the first, a YAC clone is found to be distal to the breakpoint, indicated by a hybridization signal on the normal chromosome 7 and derivative chromosome 20. Secondly, a YAC clone lying proximal to the breakpoint, indicated by a signal on the normal chromosome 7 and the derivative chromosome 7. The third outcome would be detection of a YAC clone spanning the translocation, in which hybridization signals would be detected on the normal chromosome 7 as well as both derivative chromosomes. Since somatic cell hybridization was no longer possible, FISH provided the most direct means of localizing genomic clones from the 7q32 region relative to UF53's translocation breakpoint. The ultimate goal of such FISH experiments was localization of the translocation to one YAC.

As an initial step in my positional cloning effort, as described in this chapter, I used FISH to position several YAC clones proximal and distal to the 7q32.1 translocation breakpoint in UF53 and successfully identified a YAC clone that spanned the translocation. These results placed the translocation breakpoint on a more highly resolved physical map, on the genetic map, and narrowed the candidate gene region to approximately 1 Mb.

Materials and Methods

YAC clones and DNA markers. The chromosome 7-specific YAC clones were provided by our collaborators Dr. Lap-Chee Tsui and Dr. Stephen W. Scherer (Hospital for Sick Children, Toronto). These clones were isolated from a chromosome 7-specific YAC library (Scherer et al., 1992) by screening with the microsatellite markers listed in Table 2.1. Information about the microsatellite markers can be found in the Genome Database (GDB). The unpublished Généthon microsatellite marker AFMa125wh1 was provided by Dr. Jean

Weissenbach. The Toronto group determined the sizes of the YACs by pulsed-field gel electrophoresis of the yeast chromosomes followed by blot hybridization with a vector specific probe (pBR322) and comparison to YPH149 *S. cerevisiae* chromosome standards (Scherer and Tsui, 1991).

Alu PCR. Yeast containing chromosome 7 YACs was grown in YPD medium to a density of 2×10^7 cells/ml (Scherer et al., 1993). The cells underwent spheroplasting using the Yeast Cell Lysis Preparation Kit (BIO 101), and high molecular weight DNA was prepared using the G NOME™ DNA Kit (BIO 101). The isolated DNA was phenol-chloroform extracted, ethanol precipitated and dissolved in TE. In order to generate labeled probes specific to the chromosome 7 YAC, 20-30 ng of purified DNA from each YAC clone were subjected to inter-*Alu* PCR under conditions described by Tagle and Collins (1992) using combinations of *Alu* element and YAC vector primers (Brooks Wilson et al., 1990; Lengauer et al., 1992; Riley et al., 1990; Tagle and Collins, 1992).

FISH. Five-hundred ng of combined inter-*Alu* and *Alu*-vector PCR products were biotinylated by random priming using the BioPrime™ DNA Labeling System (Gibco BRL). Approximately 100-150 ng of biotinylated DNA were used as a probe for each slide. Peripheral lymphocyte and lymphoblastoid chromosome spreads were freshly prepared by standard cytogenetic procedures (Yunis, 1976). The biotinylated YAC probe was simultaneously hybridized to the slides with digoxigenin-labeled alpha-satellite centromeric probes for chromosomes 7 and 20 (Oncor), using Cot-1 DNA competition (Pinkel et al., 1986). Slides were hybridized for approximately 16 hours at 37°C. Post hybridization washes consisted of one 1XSSC (0.01 M NaCl, 0.3 M sodium citrate, pH 7.0) wash at 72°C for 5 minutes followed by three consecutive washes in 1XPBD (Oncor) for 3 minutes at room temperature. Signal detection was attained by incubation with fluorescein isothiocyanate-conjugated (FITC) avidin and anti-

digoxigenin (Oncor). One round of signal amplification, using anti-avidin/FITC-avidin, was also carried out. Chromosomes were counterstained with propidium iodide (Oncor). The hybridization signals were analyzed and documented with an Olympus BHS fluorescence microscope system and the CytoVision/CytoProbe computer imaging device (Applied Imaging, Inc.) in collaboration with Brian A. Gray and Dr. Roberto Zori (Raymond C. Philips Unit, University of Florida).

Results

Localization of the translocation breakpoint at 7q32.1 using FISH. *Alu* PCR products from eleven YAC clones (HSC7E61, HSC7E67, HSC7E451, HSC7E1351, HSC7E888, HSC7E77, HSC7E81, HSC7E117, HSC7E591, HSC7E135, HSC7E5), from locations throughout the long arm of chromosome 7, were initially used as probes in FISH mapping experiments to determine their locations relative to the UF53 translocation breakpoint. Examples of the hybridization signals are shown in Figure 2.3 and the results are summarized in Table 2.1.

HSC7E1351 and HSC7E244, which were previously mapped to the 7q32 region (Kunz et al., 1994), were determined by FISH to be proximal (centromeric) and distal (telomeric), respectively, to the translocation breakpoint (Table 2). These two clones were also linked within a contig of fourteen YACs anchored by the microsatellite markers AFM323wd5 (D7S686), AFMa125wh1, AFM309yf1 (D7S680), AFM218xf10 (D7S514) and AFM206xc1 (D7S635) (Figure 2.4). The contig spans approximately 3 Mb (Figure 2.4) and the genetic distance between D7S686-(D7S680-D7S514-D7S635) is 1 cM (Gyapay et al., 1994).

To refine the localization of the translocation breakpoint within the YAC contig, *Alu*-PCR products from four additional YACs in the contig were tested by

Figure 2.3. FISH analysis of the SLOS translocation breakpoint region using YAC clones from the 7q32 region. Biotin-labeled *Alu* PCR products from the YACs (yellow) were cohybridized with digoxigenin-labeled alpha satellite centromeric probes for chromosome 7 and 20 (yellow) to metaphase chromosomes, under competitive conditions. Metaphase spreads of U153 lymphocytes after hybridization with the YAC clones (a) HSC7E451, (b) HSC7E1289, and (c) HSC7E261 demonstrate proximal, spanning and distal positioning of probes, respectively. Metaphase spread of an unaffected individual (d) hybridized with HSC7E1289 serves as a control. Chromosomes are counterstained with propidium iodide. Arrows point to the centromeric signals specific for chromosomes 7 and 20.

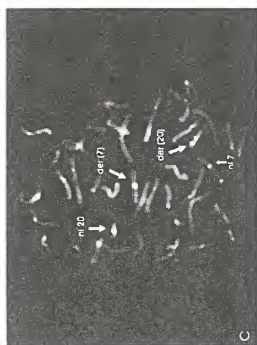
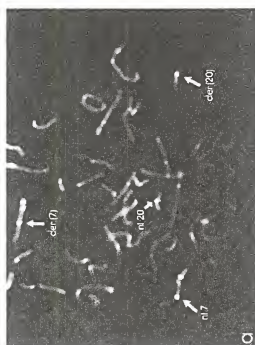
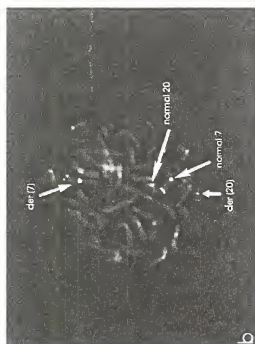


Table 2.1. Summary of FISH Experiments Using YACs

YAC Clones	^a Map Location on chromosome 7	Size (kb)	DNA Markers Contained within YAC	^b Location Relative to the Translocation Breakpoint
HSC7E61	7q21.2-q21.3	460	D7S558, D7S646, D7S657, D7S689	Proximal
HSC7E67	7q32	360	D7S648	Proximal
HSC7E451	7q32	590	D7S487, D7S648	Proximal
HSC7E1351	7q32	1,200	D7S686, AFMa125wh1	Proximal
HSC7E1289	7q32	1,800	D7S686, AFMa125wh1, D7S680, D7S514	Spans
HSC7E261	7q32-q33	580	D7S514, D7S635	Distal
HSC7E476	7q32-q33	700	D7S514, D7S635	Distal
HSC7E888	7q32-q33	410	D7S514	Distal
HSC7E244	7q32-q33	680	D7S680, D7S514, D7S635	Distal
HSC7E77	7q33	380	HBNF	Distal
HSC7E81	7q33	350	HBNF	Distal
HSC7E117	7q33-q34	480	TCRB	Distal
HSC7E591	7q33-q34	580	TCRB	Distal
HSC7E135	7q36	1,300	----	Distal
HSC7E5	7q36	300	D7S104	Distal

^aThe chromosome locations of the (HSC7E)-YACs were determined by FISH in this study or in another study (Kunz et al., 1994).

^bProximal = signals observed proximal to the breakpoint (retained on der 7); distal = signals observed distal to breakpoint (transferred to the chromosome 20 translocation derivative); and spans = probe spans the breakpoint (signals were observed on both translocation derivatives)

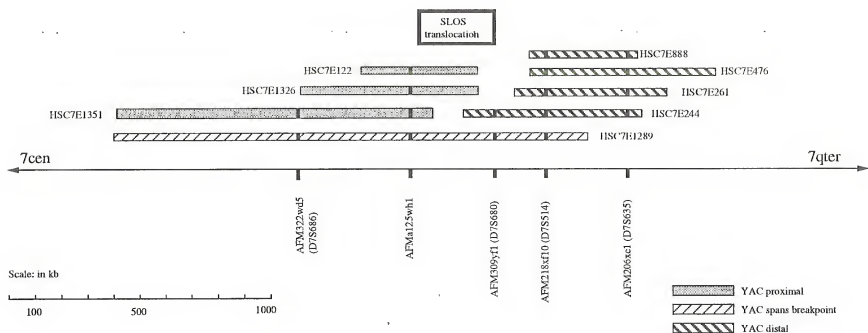


Figure 2.4. Tentative map of YACs overlapping HSC7E1289, which is known to span the translocation breakpoint. YAC locations relative to breakpoint were based on FISH data, according to the key. The YACs represented are considered nonchimeric, since the marker data are consistent, and the YACs were derived from a chromosome 7 library in which chimerism is unusual (Kunz et al., 1994). Genetic markers used to determine overlaps are listed below the line. FISH results suggest that the translocation most likely falls between markers AFMa125wh1 and AFM309yf1, as indicated by the box.

FISH. Three of the YACs (HSC7E888, HSC7E261, HSC7E476) appeared to be distal to the breakpoint (Table 2 and Figure 2.4). However, HSC7E1289 was found to span the breakpoint since in addition to a signal on the normal chromosome 7, the probe also yielded signals on both translocation derivatives (Figure 2.3). The combination of the FISH results from the other YACs suggested that the *SLOS* breakpoint lies in the telomeric half of HSC7E1289 (Figure 2.4). The results unequivocally supported the karyotyping results that placed the UF53 translocation breakpoint (and presumably *SLOS*) at 7q32.1.

Discussion

The existence of an *SLOS* patient with a *de novo* balanced translocation suggested a direct association between the chromosomal abnormality and the syndrome. The UF53 translocation served as a landmark in my initial search for the *SLOS* gene. I identified an 1,800 kb YAC, HSC7E1289, that spans the translocation breakpoint, moving the level of map resolution for this translocation from the cytogenetic band to the megabase-level.

Due to the large size of HSC7E1289, steps were taken to narrow the region of the breakpoint. HSC7E1351 and HSC7E244, which overlap HSC7E1289, mapped proximal and distal, respectively, by FISH. These results tentatively placed the breakpoint (i.e. *SLOS* gene) between markers AFMa125wh1 and AFM309yf1 (Figure 2.4). It should be noted, however, that the *Alu*-PCR FISH approach yielded results of a qualitative nature. Since *Alu* element distribution in the genome is nonuniform and was unknown within these YACs, the *Alu* PCR probe fragments may not have been representative of the entire YAC; thus, lack of signal on one or the other derivative chromosome may have been a false negative signal. To counter this, the probes included vector-*Alu* PCR products (present for most of the YACs) to help represent the YAC ends in the probe

mixture, but this does not guarantee observable signal from the ends. Other false negative signals could have been the result of a microdeletion at the breakpoint, for which there is currently no evidence. Therefore, I could not yet exclude the breakpoint from a larger region of HSC7E1289, and the conservative estimate of the SLOS breakpoint region was approximately 1 Mb.

The wide phenotypic spectrum of SLOS had traditionally caused a dilemma in clinical diagnosis; it was thought that many cases of SLOS were not appropriately diagnosed and were categorized under the nonspecific label of multiple congenital anomalies/mental retardation syndrome. SLOS, previously viewed as an uncharacterized, difficult-to-diagnose rare autosomal recessive disorder, was seen in a new light with the discovery of the aberrant sterol profile. However, the biochemical findings may not be exclusive to SLOS, and there may be biochemical or genetic heterogeneity. Clearly, for clinical purposes and development of effective therapies, where correct diagnosis is crucial, it is very important to elucidate the gene(s) involved in SLOS. Thus, at this point in my work, identification of the UF53 SLOS gene, presumably at the site of the translocation, was my goal. Localization of the UF53 translocation breakpoint was the first significant step toward this goal.

CHAPTER 3

PHYSICAL MAPPING OF THE TRANSLOCATION BREAKPOINT REGION

Introduction

Prior to my arrival in Dr. Margaret Wallace's laboratory, a collaboration with Dr. Lap-Chee Tsui at the Hospital for Sick Children (Toronto, Ontario) was established based on his involvement in the Human Genome Project, mapping chromosome 7. After narrowing the UF53 translocation breakpoint region to 200-300 kb by FISH, significant steps toward physical mapping of the region and identification of genes in the region needed to be taken. Dr. Tsui, Dr. Wallace, and I felt that the techniques and resources available in Dr. Tsui's laboratory would expedite the identification of candidate cDNAs. His laboratory was kind enough to provide me the space, resources, and their expertise for a month in 1994. This chapter includes data from experiments which I initiated while visiting Dr. Tsui's laboratory and completed upon my return to Dr. Wallace's laboratory.

The following methodologies were executed and the details of each discussed in this chapter: 1. pulsed-field gel electrophoresis to establish a rare-restriction site map of the YAC contig; 2. direct selection of cDNAs from HSC7E1326 ; and 3. FISH studies using HSC7E1289 cosmids, to continue narrowing the breakpoint region.

An extensive YAC contig was constructed, including (HSC7E)-YACs as well as CEPH-G  n  thon YACs, by Dr. Tsui's laboratory prior to my arrival. The chromosome 7-specific (HSC7E)-YAC library (Scherer et al., 1992) and CEPH-

Généthon library were screened with the polymorphic microsatellite markers specific for the 7q32 region (Kunz et al., 1994). Additional YACs thus identified were aligned with HSC7E1289 (the spanning YAC) and other YACs in the contig, based on the polymorphic microsatellite markers contained within each. The additional YACs would be used in future studies.

Construction of a physical map of the 7q32 region using PFGE established the locations of rare-restriction endonuclease sites. YAC clone DNA was digested with rare-restriction endonucleases, and the fragments were separated by PFGE and Southern blotted. Restriction maps of the YAC clones were constructed by sequential hybridizations of the PFGE blots to probes derived from the YAC ends. Autoradiography patterns revealed the positions of the rare-restriction sites in the overlapping YAC clones. These data simultaneously revealed the locations of two CpG islands, which serve as potential landmarks for constitutively expressed genes.

A relatively new methodology, direct selection, was used to identify cDNAs encoded by the region. Direct selection is particularly useful and efficient in screening large DNA fragments, even those greater than 1.0 Mb (Parimoo et al., 1991). As illustrated in Figure 3.1, the selection process is based on hybridization of cDNA fragments to immobilized cloned genomic DNA and recovery of the selected cDNAs by PCR (Rommens et al., 1994). Direct selection begins with the production of cDNAs from reverse transcription of total and poly-A⁺ RNA from various tissues, using primers with specific sequence tags for each tissue. These cDNAs are pooled and expanded by PCR. The YACs are isolated from pulsed-field gels and transferred to a filter. Occasionally, due to size overlap, it is impossible to separate the YAC from a yeast chromosome, a disadvantage overcome by subsequent negative selection with yeast genomic

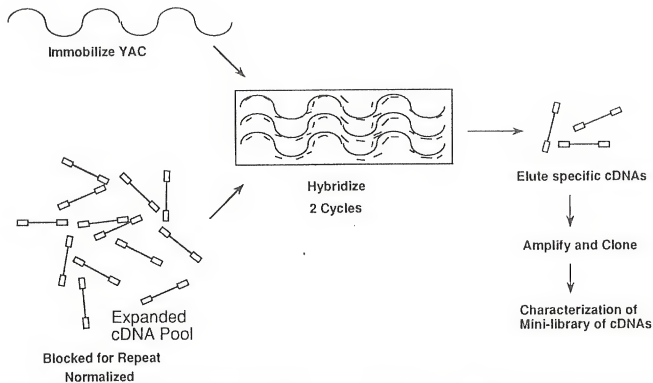


Figure 3.1. Schematic of basic direct selection strategy (Rommens et al., 1994). The pool of expanded cDNAs is competed with repetitive DNA and hybridized with the immobilized genomic DNA. The membrane is washed and the cDNA eluted off. These cDNAs are again competed with repetitive DNA and rehybridized to the membrane. The membrane is once again washed and the cDNAs eluted and amplified by PCR. The PCR products are subsequently cloned into a plasmid vector and characterized.

DNA. Prior to the hybridization, competition with repetitive DNA is necessary; competition against either the cDNA pool or the immobilized YAC works equally well (Lovett, 1994). The cDNA pool is then hybridized with the filter, after which the filter is washed and the bound cDNAs are eluted. The eluted cDNAs are again competed and rehybridized to the same filter followed by elution. These highly-enriched, selected cDNAs are amplified by PCR and shotgun subcloned into a vector, followed by transformation into competent *E. coli* cells. Clones are then analyzed for content of repetitive elements, yeast DNA or human genomic DNA (i.e. false positive background clones) (Parimoo et al., 1993). Prior to my arrival in Toronto, direct cDNA selection from HSC7E1326 was initiated by Dr. Joanna Rommens in collaboration with Dr. Tsui's laboratory. I was responsible for the analysis of the direct selected cDNA clones to determine whether they contained yeast or human genomic DNA. I was also involved in localizing the human cDNA clones on the YAC contig using Southern analysis.

Additionally, in a parallel positional cloning strategy, the Genome Data Base (GDB) and literature were searched for potential candidate genes. Initial candidate genes included all genes and uncharacterized cDNAs in 7q32, even if their relationship to cholesterol metabolism was unknown. This "positional candidate" approach has been used successfully to identify the genes for hereditary hemorrhagic telangiectasia (McAllister et al., 1994) and achondroplasia (Shiang et al., 1994), among others. This strategy can save significant effort, although it relies on good fortune. Literature review revealed that the *PAX4* gene maps to same general region as the translocation breakpoint. *PAX4* is one of nine genes belonging to the PAX family of homeobox genes. This family encodes nuclear transcription factors involved in developmental control during embryogenesis in both vertebrates and invertebrates (Stuart and Gruss, 1995). *PAX4* was originally mapped to chromosome 7 in 1993 (Stapleton et al.,

1993) and then regionally mapped to the chromosome band 7q32 by FISH a year later (Tamura et al., 1994). The *PAX4* gene was later found to reside approximately 500 kilobases distal to the UF53 breakpoint. Due to its close proximity to the translocation breakpoint and its ubiquitous involvement in transcriptional regulation during embryogenesis, investigation into its possible involvement in SLOS was warranted. Although *PAX4* was clearly not directly disrupted by the translocation, it was conceivable that the expression of this gene could be influenced by a position effect similar to that described in aniridia (which involves another family member *PAX 6*.) (Fantes et al., 1995) and campomelic dysplasia (Foster et al., 1994; Schafer et al., 1995). In both disorders, the causative genes are positioned 100-200 kb from translocation breakpoints. One explanation for positional effect is that the gene rearrangement leads to an inappropriate chromatin environment for normal gene expression (Foster et al., 1994). Since position effect was difficult to investigate, I set aside further analysis of *PAX4* while searching for other genes closer to the breakpoint.

Also, during my visit, a partial cDNA of the *mGluR8* gene (Duvoisin et al., 1995) was serendipitously mapped to the human 7q32 region. *GRM8*, the human homolog of *mGluR8*, a novel member of the metabotropic glutamate receptor gene family, was found to lie on HSC7E1289; however, the genomic structure, cDNA sequence, and expression pattern of this gene had not been determined (Scherer et al., 1996). Please note the difference in nomenclature between the mouse and the human homologs: the mouse gene is referred to as *mGluR8* while the human gene is referred to as *GRM8*. While the partial *GRM8* cDNA probe clearly mapped significantly centromeric to the breakpoint, it was unknown if its genomic sequence was disrupted by the translocation. Although this gene was not known to be involved in cholesterol synthesis, it was unclear if its disruption could contribute to the SLOS phenotype. Thus, *GRM8* became the

top candidate gene in the region and was further analyzed as described in Results.

Materials and Methods

Large scale preparation of YAC PFGE blocks. One-hundred ml of YPD (1% bacto yeast extract, 2% bacto peptone, 2% dextrose, pH 5.8) media with 100 µg/ml ampicillin was inoculated with a 5-10 µl of a YAC glycerol stock and incubated overnight at 30°C. Cultures were centrifuged at 2000 rpm for 5 minutes at 20°C, supernatant decanted, and the pellet resuspended in 4 ml SCE (1.0 M sorbitol, 0.1 M sodium citrate, 0.06 M EDTA). To this suspension, 2 µl of β-mercaptoethanol and 50 µl lyticase (100 units/ml) were added and mixed. An equal volume of molten (50°C) 1% SeaPlaque® GTG agarose (FMC BioProducts) in 50 mM EDTA was added and mixed. This mixture was poured onto a glass plate and allowed to cool for 15 minutes at room temperature and 15 minutes at 4°C. The agarose was cut into appropriate sized blocks (approximately 5 mm X 10 mm), transferred to 20 ml SCEM (SCE + 0.2% β-mercaptoethanol), and incubated at 37°C overnight while gently shaking. The YAC blocks were washed with lysis buffer (100 mM EDTA, 10 mM Tris-Cl, at pH 7.5) three times to rinse away debris, followed by an overnight incubation in 20 ml lysis buffer with 1 mg/ml Proteinase K at 37°C with gentle shaking. The blocks were then dialyzed with 50 mM EDTA, 3 times over a period of 1-2 hours. Blocks were transferred to fresh 50 mM EDTA and stored at 4°C.

Partial digest of YAC blocks with rare-restriction endonucleases.

Individual YAC blocks were placed in eppendorf tubes containing serial dilutions (1:0, 1:10, 1:50) of the restriction endonucleases BssHII, MluI, or NotI, 10 µl appropriate 10 X buffer, and sterile distilled water in a final volume of 100 µl. These were incubated on ice for 30 minutes, followed by incubation at the

appropriate temperature (50°C for BssHII and 37°C for MluI and NotI) for a minimum of 3 hours. The digestions were stopped with the addition of 50 mM EDTA.

PFGE of YAC blocks. Digested YAC blocks were loaded into the lanes of a 1/2 X TBE 1% agarose gel in 1/2 X TBE buffer. The gel was run in a BioRad CHEF DRII hexagonal field unit, at 4°C, ramping from 20 seconds per electrode to 40 seconds per electrode evenly over 20 hours at 200 volts. DNA was transferred to a nylon membrane using standard Southern methodology (Sambrook et al., 1989). The PFGE blot was hybridized with a vector-specific probe (pBR322) labeled by random-priming with α -³²P dCTP (MegaPrime kit, Amersham). Hybridization patterns were visualized by autoradiography, and band sizes were determined by comparison to YPH149 yeast chromosome standards (Scherer and Tsui, 1991).

Rapid DNA preparation from yeast. Five ml of YPD with 100 µg/ml ampicillin were inoculated with 5-10 µl YAC glycerol stock and incubated overnight at 30°C. The cells were pelleted at 2000 rpm for 5 minutes, the supernatant removed, and the pellet resuspended in 500 µl sterile distilled water and transferred to an eppendorf tube. The cells were pelleted by microcentrifugation and the supernatant removed. To the cells, 200 µl of GDIS (2.0% Triton-X-100, 1.0% SDS, 100 mM NaCl, 10 mM Tris-Cl (pH 8.0), 1 mM EDTA), 200 µl phenol-chloroform:isoamyl alcohol (24:1), and .35 grams of heat-treated glass beads were added to the cell suspension and vortexed for 2.5 minutes. To this mixture, 200 µl sterile distilled water were added, mixed, and then microcentrifuged for 1 minute. The aqueous layer was transferred to a fresh eppendorf tube containing 6 µl RNase A (10 mg/ml) and incubated at room temperature for 30 minutes. The DNA was then ethanol precipitated and resuspended in 100 µl sterile distilled water.

Southern blot analysis of 7q32 YACs with *mGluR8*, *mGluR8* selected cosmids, and direct selected cDNAs. Purified genomic DNA from the YAC clones from the chromosome 7-specific YAC library or the CEPH-G  n  thon YAC library (Figure 3.2) were subjected to restriction endonuclease digestion with EcoRI. The restriction fragments were separated on a 1% agarose gel and transferred to a nylon membrane by standard protocol (Sambrook et al., 1989). The full-length *mGluR8* cDNA (kindly provided by Dr. Duvoisin), unique cosmid sequences (described below), and direct selected cDNAs were labeled by random-priming with α -³²P dCTP (MegaPrime kit, Amersham) for individual hybridization against YAC blots. Hybridization and wash conditions were based on a version of the Church and Gilbert SDS/sodium phosphate method (Church and Gilbert, 1984).

Identification of unique sequence fragments from the *mGluR8* cosmids. The full-length *mGluR8* cDNA was used to screen a human chromosome 7-specific cosmid library to identify cosmids presumably containing exons of the *GRM8* gene. The screening, done in Toronto, resulted in the retrieval of 16 cosmids. The bacterial strains containing the cosmids were grown in 100 ml Luria broth with 25  g/ml kanamycin overnight in a 37  C orbital shaker. The cosmid DNA was then purified according to the Qiagen Plasmid Midi Kit protocol. Each cosmid (200 ng) was digested with EcoRI, with the fragments separated on a 1% agarose gel and transferred to a nylon membrane (Sambrook et al., 1989). The cosmid blot was hybridized with total human genomic DNA (50 ng) labeled by the random-priming with α -³²P dCTP (MegaPrime kit, Amersham). Bands were visualized by autoradiography. Fragments containing unique (non-repetitive) sequence were identified by the absence of hybridization with total human genomic DNA, and were isolated according to the QIAEX II protocol (Qiagen).

Double digest of GRM8 cosmids. Cosmid DNA was extracted as described above. Each cosmid (500 ng) was digested with the restriction endonuclease EcoRI at 37°C for 1 hour. The digested DNA was ethanol precipitated and resuspended in 1XTE. Three 100 ng aliquots of the EcoRI digestion were then digested with the rare-restriction endonucleases BssHII, MluI, or NotI for an additional hour. The fragments were then separated on a 1% agarose gel, stained with ethidium bromide and visualized on a UV light box.

Results

Completion of 7q32 the YAC contig. Prior to my arrival in Toronto, screening of the chromosome 7-specific (HSC7E) YAC library and CEPH-Généthon YAC library with the 5 polymorphic microsatellite markers contained in HSC7E1289 (refer to Figure 2.2) and two new Généthon markers, AFMa065zg9 and D7S1801, resulted in the recovery of 16 YACs. These additional YACs were aligned with HSC7E1289 based on their marker content, resulting in an expansive 7q32 contig composed of 24 overlapping YACs (Figure 3.2). This construction of a more complete YAC contig was intended to facilitate more precise positioning of various clones and cDNAs recovered from other studies.

Establishment of rare-restriction sites in the 7q32 YAC contig by PFGE. Using restriction endonucleases that recognized rare restriction sites, PFGE produced a physical map of the YAC clones (HSC7E1289, HSC7E122, c752c8, HSC7E476, HSC7E261, and HSC7E244) surrounding the translocation breakpoint (Figure 3.3). A CpG island consisting of two BssHII sites, one MluI site and one NotI site, was identified distal to the translocation on the telomeric end of HSC7E1289. An additional CpG island was also identified at the distal end of the contig not contained in HSC7E1289. Of particular interest, though, was the

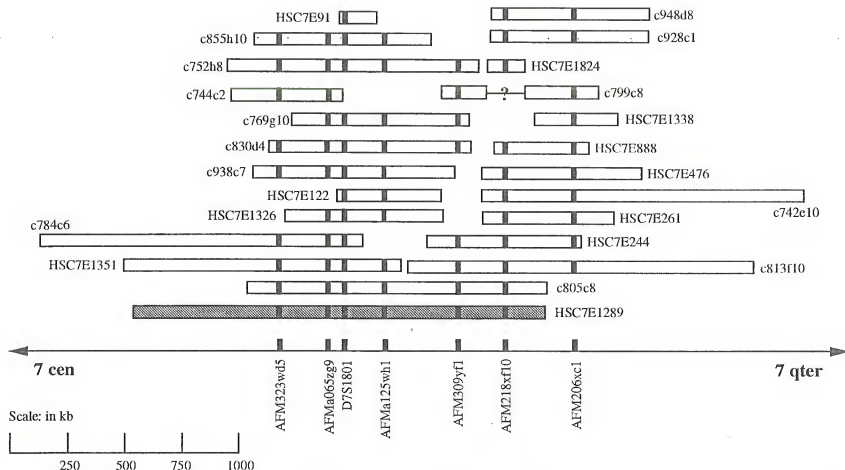


Figure 3.2. Expanded map of the 7q32 YAC contig. The (HSC7E)-YACs were obtained from a chromosome 7-specific YAC library (Scherer et al., 1992) and the CEPH YACs were obtained from the CEPH-Généthon YAC library. The five original microsatellite markers, as well as two additional Généthon markers, were used to align the YACs (markers indicated by black vertical bars): YAC HSC7E1289 found to span the UF53 breakpoint by FISH, is shaded.

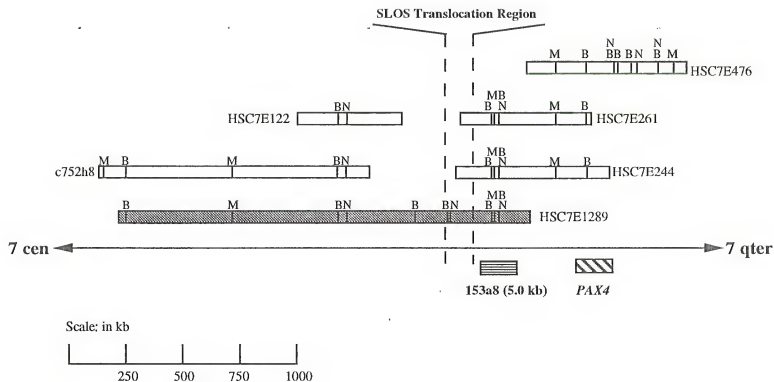


Figure 3.3. Physical map of the translocation region at 7q32. The YACs (open and stippled boxes) are drawn to scale and show the rare-restriction sites established from PFGE analysis: B=BssHII, M=MluI, and N=NotI. The cosmid 153a8 (horizontally striped box) and the *PAX4* gene (diagonally striped box) were placed on the map by hybridization against Southern blots of the YACs. The complete distribution of the *GRM8* gene on HSC7E1289 is currently unknown and is thus not indicated on the map. 153a8 and *PAX4* are not to scale.

mapping of a partial *GRM8* cDNA to the centromeric end of HSC7E1289.

Southern blot analysis of 7q32 YACs with full-length *GRM8* cDNA.

Hybridization of the 7q32 YAC Southern blot with the full-length *mGluR8* cDNA showed hybridization across a large span of the YAC contig (Figure 3.4). The lane containing HSC7E1289 DNA showed at least 6 EcoRI bands ranging from 3 to 12 kb in size. More interesting, though, was the detection of bands in YAC clones known to fall proximal (HSC7E1326 and HSC7E1351) and distal (HSC7E244 and HSC7E122) to the translocation based on FISH studies. Several of the CEPH-G  n  thon YACs, both centromeric and telomeric in the contig, had similar banding patterns as those seen in the YACs from the FISH studies. Two CEPH-G  n  thon YACs (c963f9 and c897c6) from outside the 7q32 region served as controls for yeast cross-hybridization, YAC vector hybridization, or nonspecific hybridization. The Southern analysis suggested that the *GRM8* gene contained sequences located on both sides of UF53's translocation. The *mGluR8* cDNA was used to screen a chromosome 7 cosmid library from which 16 cosmids were retrieved. These *GRM8* cosmids were positioned on the contig by Southern blot analysis.

Localization of unique sequence fragments from *GRM8* cosmids on the 7q32 YAC contig. Hybridization of the unique sequence fragments against YAC contig Southern blots placed all of the cosmids within 1 Mb on the contig. Relative placement was based on the presence or absence of a hybridization signal(s) in overlapping YACs (demonstrated in Figure 3.5). A hybridization signal of the same size, present in all lanes, was concluded to be cross hybridization of the residual cosmid vector sequences in the probe to the YAC vector. This crude localization also established that all of the cosmids were contained within HSC7E1289, the YAC spanning UF53's translocation. One cosmid, 153a8, was localized near the telomeric end of HSC7E1289 while the

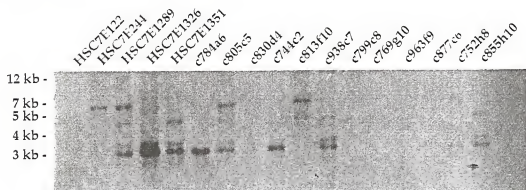


Figure 3.4. Southern blot analysis of the YACs from the 7q32 contig hybridized with the full-length *mGluR8* cDNA to determine the genomic span of *GRM8*. The Southern blot was composed of the (HSC7E)-YACs used in the FISH studies and CEPH YACs which overlapped with HSC7E1289, with the exception of c963f9 and c897c6 which served as controls. Fragment sizes indicated to the left of the panel were based on Gibco-BRL's 1 kb ladder.

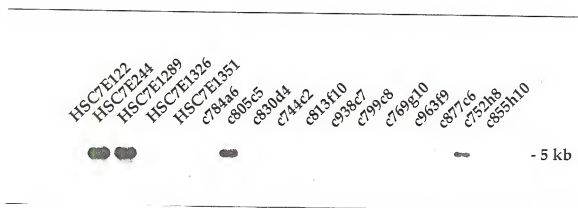


Figure 3.5. Southern blot analysis of the YACs from the 7q32 contig hybridized with a 5.0 kb *EcoRI* fragment from the *GRM8* cosmid 153a8. The 5.0 kb fragment was chosen based on its lack of repetitive sequences. This experiment indicated the relative location of this cosmid on the YAC contig.

most centromeric cosmids, 13e6 and 192d4, were localized approximately 1 Mb from 153a8 (Figure 3.6). Since 153a8 was localized to the same region of HSC7E1289 as the CpG island, it was further analyzed for the presence of a CpG island.

Identification of a CpG island in the GRM8 cosmid 153a8. The double digests of the GRM8 cosmids with EcoRI and BssHII, MluI, or NotI established that only one cosmid contained a putative CpG island. At least two BssHI sites, two MluI sites, and one NotI site were found to be contained within cosmid 153a8 (Figure 3.7). The relative placement of 153a8 on the YAC contig and the existence of a CpG island in this cosmid strongly suggested that the CpG island on the distal end of HSC7E1289 and the CpG island contained in 153a8 were one and the same. Furthermore, 153a8's hybridization to the *mGluR8* cDNA suggested that this CpG island likely represented the 5' end of the GRM8 gene.

Discussion

Following the identification of YAC HSC7E1289 spanning UF53's translocation, experiments were undertaken to further narrow the translocation breakpoint and to identify genes in the region. Since the rate of progress and success of any one positional cloning approach was unpredictable, several approaches were concurrently pursued to insure that cDNAs would ultimately be identified. The direct selection of cDNAs from HSC7E1326 was an unsuccessful approach. Approximately 200 clones were recovered from the direct selection of HSC7E1326. Of these 200, I isolated fifty of the inserts which were hybridized against the YAC Southern blots, and found that approximately 80% of the clones were false positives containing repetitive sequence (data not shown). It was predicted that 70-140 unique sequence, direct-selected cDNAs should have been isolated from HSC7E1326 based on its 700 kb size

HSC7E1289

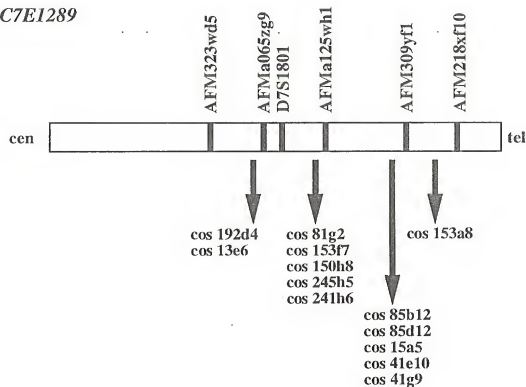


Figure 3.6. Schematic representation of location of thirteen of the *GRM8* cosmids along *HSC7E1289*. The arrows indicate the relative positions of the cosmids with respect to the DNA markers (denoted by the black vertical bars). The positions of the cosmids were established by Southern blot analysis of YACs from the 7q32 contig. For simplicity, only *HSC7E1289* is included in this illustration. Cosmid 153a8 cross hybridized with the 5' end of the *mGluR8* cDNA, suggesting that the 5' end of *GRM8* lies toward the telomere.

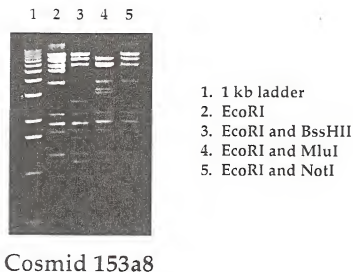


Figure 3.7. Restriction digests of the *GRM8* cosmid 153a8. Cosmid 153a8 was digested with EcoRI alone (lane 2) and double digested with EcoRI and BssHII, MluI, or NotI (lanes 3-5). Ethidium bromide-staining of the 1% agarose gel revealed the loss of several EcoRI bands and the subsequent appearance of new smaller bands as a result of the double digestion with the above rare-restriction endonucleases. The molecular weight marker is Gibco-BRL's 1 kb ladder (lane 1).

(Rommens et al., 1994). Due to the lack of unique cDNA clones in this experiment, it was suggested that HSC7E1326 was rich in repetitive sequences (Dr. Joanna Rommens, Toronto, personal communication). Further analysis of the few unique clones was abandoned, as well as direct selection using other 7q32 YACs, after the discovery that *GRM8* was putatively interrupted in UF53 (discussed below).

Throughout the human genome, the cytosines in CpG dinucleotides are typically methylated, with the exception of a small percentage of unmethylated CpG's which occur in discrete "islands" (Bird et al., 1987). These islands, now known as CpG islands, are defined as regions of DNA, usually more than 200 bp long, with a GC-content greater than 50% (Larsen et al., 1992). The number of CpG islands in the haploid human genome is estimated to be approximately 30,000 (Bird, 1986). In studies by Larsen et al. in 1992, 50% of the genes analyzed were associated with CpG islands, with a majority of this fraction representing housekeeping and other ubiquitously expressed genes. The CpG islands associated with these particular genes began 5' to the transcription initiation site, included one or more exons and introns, and usually included the promoters. Additionally, 40% of tissue-specific expressed genes and other genes with limited expression were associated with CpG islands. In these cases, CpG islands were not biased to the 5' end of the transcription unit. Some CpG islands were shown to encompass bi-directional promoters, implying that a single CpG island could be associated with two genes (Poschl et al., 1988).

Physical mapping of the YAC contig using PFGE and rare-restriction endonucleases established the presence of two CpG islands. The first CpG island was located on the telomeric end of HSC7E1289, while the other was found approximately 0.5 Mb distal on the contig. As shown in Figure 3.3, the second CpG island corresponded to the *PAX4* gene, which was placed on the map by

hybridization of YAC Southern blots with a mouse cDNA clone, provided by Peter Gruss, Max Planck Institute, Germany (Dr. Steve Scherer, personal communication). Of greater importance, though, was the presence of the CpG island on the telomeric end of HSC7E1289, which lay distal to the breakpoint. Since CpG islands are almost always associated with genes, the presence of the CpG island on distal HSC7E1289 implied that a gene was in close proximity.

The most pivotal experiment performed during my visit to Dr. Tsui's laboratory was the Southern blot analysis of the 7q32 YACs with the full-length mouse *mGluR8* cDNA. Initially, *GRM8* was not viewed as a potential candidate gene based on the fact that it had no apparent connection with cholesterol metabolism and appeared to map quite proximal to the translocation breakpoint. But since the full span of the gene was not known, I convinced the Tsui laboratory that we needed to pursue full mapping of this gene. Thus, I hybridized the full-length *mGluR8* cDNA against the YAC Southern blots to test this gene's distribution on the contig. Fortuitously, the *mGluR8* cDNA hybridized to YACs known to fall proximal and distal to UF53's translocation. The Southern blot patterns observed in HSC7E1289 and the overlapping YACs (HSC7E1351, HSC7E1326, HSC7E122, HSC7E244, c784a6, c805c8, c830d4, c744c2, c813f10, c938c7, c752h8 and c855h10) indicated that the *GRM8* gene was distributed along the central portion of the contig, and could possibly span the breakpoint. Although these original data were not completely conclusive, further investigation into the relative position of the *GRM8* gene to the translocation was warranted.

At the time of these studies, no cDNA or genomic sequence information existed for the human *GRM8* gene. Further experimentation required human *GRM8* cDNA or genomic clones. Thus, as mentioned previously, a human chromosome 7 cosmid library was screened with the full-length *mGluR8* cDNA

and 16 cosmids retrieved. To quickly place the cosmids on the physical map, unique sequences were isolated from each cosmid and individually hybridized against the YAC Southern blots (Figure 3.5). The relative locations of the *GRM8* cosmids to HSC7E1289 are represented in Figure 3.6. The cosmids were localized along a 700 kb section of HSC7E1289 between the markers AFM323wd5 and AFM218xf10. The physical mapping of the cosmids, coupled with my earlier FISH studies tentatively placing UF53's translocation between markers AFMa125wh1 and AFM309yf1, strengthened the argument for further investigation of the *GRM8* gene.

Rare restriction site analysis of the *GRM8* cosmids shed further light on the relative location of one cosmid on the physical map, establishing the existence of a CpG island in the cosmid 153a8 (Figure 3.7). Southern blot analysis of this particular cosmid placed it on the YAC contig at the same location as the CpG island established by PFGE (Figure 3.3 and Figure 3.6). Collectively, these results confirmed that the CpG island found in the YAC contig near the distal end of HSC7E1289 was also contained in the *GRM8* cosmid 153a8. These preliminary data suggested that the *GRM8* gene was most likely disrupted by the translocation in UF53. Confirmation of these preliminary data would come from FISH studies with the *GRM8* cosmids.

CHAPTER 4

IDENTIFICATION OF A METABOTROPIC GLUTAMATE RECEPTOR GENE (*GRM8*) DIRECTLY DISRUPTED BY UF53'S TRANSLOCATION

Introduction

Since *GRM8* became the key candidate gene in the translocation region, it was important to review the known roles of glutamate receptors in order to better evaluate *GRM8* as a possible *SLOS* gene. Glutamate not only serves as the major neurotransmitter in the central nervous system (CNS) of all mammals but also plays a vital role in neuronal plasticity, as exemplified by long-term potentiation (LTP) and long-term depression (LTD), and neuronal toxicity (Nakanishi, 1992; Tanabe et al., 1992). Glutamatergic dysfunction has been implicated in neuronal cell death following ischemia, hypoglycemia, and anoxia (Choi, 1992), in epilepsy (Rogers et al., 1994), and in neurodegenerative disorders (Thomas, 1995).

Two distinct groups of receptors are responsible for mediating the actions of glutamate: the ionotropic and metabotropic glutamate receptors. Activation of the ionotropic glutamate receptors, which are coupled to ion channels in the membrane, results in the entry of calcium and sodium ions into the cell leading to polarization of the membrane (MacDermott et al., 1986; Murphy et al., 1987; Thomas, 1995). The ionotropic glutamate receptors are divided into distinct subtypes based on their pharmacological and electrophysiological selectivity for N-methyl-D-aspartate (NMDA), alpha-amino-3-hydroxy-5-methyl-isoxasole-4-propionate (AMPA) and kainate (Monaghan et al., 1989). The metabotropic glutamate receptors are G-protein-coupled receptors which indirectly mediate

intracellular signaling through secondary signaling pathways (Knopfel et al., 1995; Scherer et al., 1996). To date, eight mGluRs have been identified and subdivided into three subfamilies based on sequence homology and pharmacological properties (Duvoisin et al., 1995).

mGluRs were first postulated to exist based on studies demonstrating that glutamate stimulation resulted in the activation of phospholipase C (PLC) via a G-protein leading to the accumulation of inositol triphosphate (IP₃) in the CNS (Sladeczek et al., 1985; Sugiyama et al., 1987). The first mGluR was cloned using a functional expression screening process (Houamed et al., 1991; Masu et al., 1991). In brief, this screening procedure made use of the secondary signaling pathway in *Xenopus* oocytes that link G-protein activation with chloride channel currents that could be electrophysiologically measured. The oocytes were injected with pools of total RNA from rat cerebellum and tested for glutamate stimulation reflected by an oscillatory chloride current response. These pools were then successively subdivided until a single clone eliciting a response, called mGluR1, was identified. The remaining family members and several splice variants were identified by using mGluR1 as a probe or using its sequence to design degenerate PCR primers to screen additional cDNA libraries (Abe et al., 1992; Duvoisin et al., 1995; Minakami et al., 1993; Nakajima et al., 1993; Okamoto et al., 1994; Pin et al., 1992; Tanabe et al., 1992). As mentioned above, the mGluRs are subdivided into three subgroups based on their sequence homology (Pin and Duvoisin, 1995). mGluR1 and mGluR5, as well as their splice isoforms, comprise Group-I, mGluR2 and mGluR3, Group-II, and mGluR4, mGluR6-mGluR8, Group-III. Within any given group, amino acid sequence homology is around 70%, where as between groups the homology falls to around 40% (Figure 4.1).

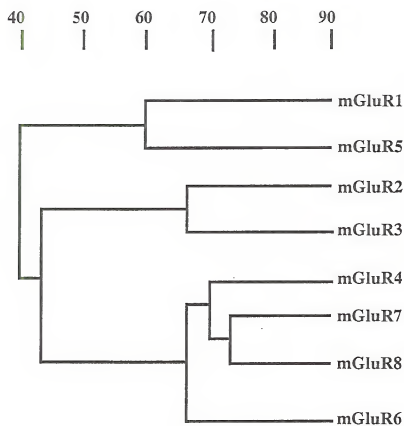


Figure 4.1. Dendrogram of the mGluR family members (Pin and Duvoisin, 1995). The number at the top indicates % amino acid identity between members of the family.

Although the mGluRs have differences in sequence, there are important predicted structural features which are consistent among the members of this family. All of the glutamate receptors have an extracellular amino terminus with a putative signal peptide, seven hydrophobic segments forming seven transmembrane domains, and an intracellular carboxy terminus as predicted by hydrophobicity analysis (Sudzak et al., 1994). The conserved regions, illustrated in Figure 4.2 using mGluR1a as an example, are evenly distributed throughout the length of the receptor. This differentiates the mGluRs from other G-protein-coupled receptors which show high conservation in the transmembrane regions. There are twenty-one cysteine residues conserved among the mGluRs; nineteen of these are located in the extracellular domain and extracellular loops in the putative ligand binding domain. The third intracellular loop, which is implicated in the functional coupling of the other receptors to G-proteins (Luttrell et al., 1993; Maggio et al., 1993; Pin and Duvoisin, 1995), has a highly conserved amino acid sequence between the different mGluR subtypes. This was an unexpected observation based on the coupling of these receptors to different secondary-signaling pathways.

Localization of the *mGluR* mRNA in the CNS has been strictly based on *in situ* hybridization using cDNA clones for the different receptor subtypes. Hybridization with the *mGluR* probes demonstrated that the cells in most of the different brain regions are positive for multiple mGluR subtypes (Sudzak et al., 1994). For example, hybridization of probes for Group-I, Group-II, and mGluR4 and mGluR7 (from Group-III), all showed positive mRNA expression in the cerebral neocortex. In addition to expression in the CNS, mGluR1, mGluR6 and mGluR8 have detectable expression patterns in the retina (Duvoisin et al., 1995; Nakanishi, 1994). The heterogeneous mGluR expression distribution in the CNS suggests that different intracellular responses are generated as a result of

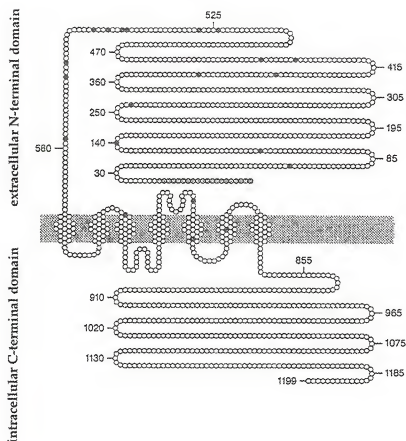


Figure 4.2. Schematic representation of the structure of mGluR1 (Huoamed et al., 1991; Masu et al., 1991). The conserved cysteine residues are represented by filled circles and the signal peptide is represented by light gray circles. mGluR1 is the largest of all described family members.

the differential expression of mGluR subtypes.

mGluRs have been shown to be directly or indirectly coupled to multiple secondary-signaling pathways involving the activation of PLC, mobilization of intracellular stores of calcium, stimulation and inhibition of adenylate cyclase, and presynaptic inhibition of glutamate release (Nakanishi, 1994; Pin and Duvoisin, 1995). Group-I receptors directly activate PLC which in turn cleaves phosphatidylinositol-4,5-*bis*-phosphate (PIP₂) into inositol-1,4,5-triphosphate (IP₃) and diacylglycerol (DAG). These then act as secondary messengers (Jeffrey Conn et al., 1994), with IP₃ causing the release of calcium from intracellular stores. The calcium ions are then free to interact with a variety of proteins which stimulate or inhibit various cellular activities. DAG, on the other hand, activates protein kinase C (PKC) in the presence of calcium. Once activated, PKC affects a variety of cellular responses involved in cell growth and metabolism. Also, the accumulation of DAG causes the release of arachidonic acid by a DAG-specific phospholipase. Both cyclooxygenase and lipoxygenase use arachidonic acid as a substrate for the production of prostaglandins and leukotrienes, respectively, which have a variety of cellular effects including the inflammatory cascade. Glutamate stimulation of Group-II and -III mGluRs induces G-protein-mediated inhibition of adenylate cyclase (Knöpfel et al., 1995). Inhibition of adenylate cyclase results in the decreased production of cyclic adenosine monophosphate (cAMP). cAMP plays an essential role in modulations of ion channels, regulation of synaptic transmission, regulation of gene expression and a multitude of metabolic functions. Thus, inhibition of cAMP can have a significant impact on the cellular activities in the CNS.

My preliminary studies implicated a metabotropic glutamate receptor gene, *GRM8*, as the putative candidate gene interrupted by the translocation in UF53. *mGluR8* was the newest member of the metabotropic glutamate receptor

family (Duvoisin et al., 1995). The receptor was identified by screening a mouse retina cDNA library with degenerate primers derived from two conserved amino acid sequences in the sixth transmembrane region and two PCR fragments encoding the seventh transmembrane region from mGluR1 and mGluR3 (Houamed et al., 1991; Tanabe et al., 1992). The deduced amino acid sequence revealed that mGluR8 had the same structural features seen in the other family members (described above). Assignment of this receptor to the Group-III subfamily was based on sequence homology to mGluR4, mGluR6, and mGluR7. *In situ* hybridization studies in mouse revealed that wide-spread *mGluR8* mRNA expression was observable throughout the CNS, retina and peripheral nervous system (PNS) at embryonic day 16. In the adult mouse, expression was limited to the olfactory bulb in the mitral/tufted cells, which are responsible for presynaptic regulation of glutamate release, and to the retina, in cell types not yet determined.

As described previously, the full-length *mGluR8* cDNA was used to screen a human chromosome 7-specific cosmid library (Duvoisin et al., 1995) and the retrieved cosmids were used in FISH experiments with UF53's metaphase spreads. The desired goal of this set of experiments was the discovery of cosmid clones falling both proximal and distal to the translocation, to confirm that the translocation interrupts *GRM8*. As described in this chapter, I identified two such cosmids (one proximal and one distal to the breakpoint) indicating that the *GRM8* gene spans a large genomic region and is interrupted by UF53's translocation.

Materials and Methods

FISH. The bacterial strains carrying the chromosome 7-specific cosmids were grown in Luria Broth supplemented with 25 µg/ml kanamycin for 16

hours. The cosmid DNA was purified (Qiagen, Maxi-Prep), and 1 µg was nick translated with digoxigenin-11-dUTP according to the Large Fragment Probe Labeling Kit protocol (Oncor). The digoxigenin-labeled DNA (50 ng) was ethanol precipitated with 50 ng human Cot-1 DNA (Gibco BRL) and resuspended in 10 µl Hybrisol VI (Oncor).

UF53 lymphoblastoid chromosome spreads were freshly prepared by standard cytogenetic procedures (Yunis, 1976). The labeled cosmid probe DNA was denatured at 72°C for 5 minutes and allowed to reanneal at 37°C for 15 minutes prior to hybridization. The chromosomes on the slides were denatured and hybridized with the probe at 37°C for at least 16 hours in a humidifying chamber. Post-hybridization washes consisted of 1XSSC at 72°C for 5 minutes followed by 1XPBD at room temperature. The chromosomes were incubated with rhodamine-conjugated rabbit anti-digoxigenin IgG (Boehringer Mannheim) for 15 minutes at 37°C, followed by three 2 minute 1XPBD washes at room temperature, and counterstained with DAPI/antifade (Oncor) to allow signal detection and chromosome identification. Subsequent analysis and documentation of hybridization signals employed an Olympus BHS fluorescence system and the CytoVision/CytoProbe computer imaging device (Applied Imaging) with the technical support of Brain Gray and Dr. Roberto Zori at the R.C. Philips Unit.

PCR Amplification of Exons 1 and 2. Dr. Stephen W. Scherer and Dr. Lap-Chee Tsui provided the preliminary sequence and primers for *GRM8* exons 1 and 2. PCR primers included the 5' end (5'-ATGTATGCGAGGGAAG-3') and the 3' end (5'-ATGTTAGCAAACCATGAT-3') of human *GRM8* exon 1, and the 5' end (5'-ATACCTCAAATTAGGCTACA-3') and the 3' end (5'-TCACCCCTCGAGAACTGGGTGAAG-3') of *GRM8* exon 2. Amplification

was performed with 100 ng of cosmid DNA, 200 ng of each primer, 0.2 mM dNTPs, 1.5 mM MgCl₂, and 0.8 U Taq polymerase in a 50 µl reaction, under standard buffer conditions. PCR conditions consisted of 35 cycles of 1 minute at 94°C, 1 minute at 65°C and 1 minute at 72°C, followed by a final 30 minute extension at 72°C. PCR products were analyzed on a 1% agarose gel and detected with ethidium bromide staining and UV illumination.

Southern blot analysis of GRM8 cosmids with exon 2. A Southern blot of the GRM8 cosmids was prepared by digestion of 500 ng of each cosmid with EcoRI, separation by gel electrophoresis on a 1% agarose gel, and transfer to Hybond N (Amersham). Twenty-five ng of the 214 bp exon 2 PCR product was labeled by random-priming with α -³²P dCTP (MegaPrime kit, Amersham) and hybridized against the GRM8 cosmid blot. Hybridization and wash conditions were based on the Church and Gilbert SDS/sodium phosphate method (Church and Gilbert, 1984). Bands were visualized by autoradiography.

Results

Identification of an Interrupted Glutamate Receptor Gene using FISH.

Nine cosmid clones (13e6, 15a5, 41e10, 85b12, 109c4, 150h8, 153a8, 153f7, 192d4) which hybridized to portions of the full-length mouse cDNA were chosen as probes in FISH experiments to determine their location relative to UF53's translocation breakpoint. Prior to FISH analysis, the cosmids were positioned relative to the full-length *mGluR8* cDNA, by our collaborators in Toronto, based on the hybridization of the cosmids to one of three cDNA fragments produced by digestion of the cDNA with EcoRI, KpnI, and MluI. Of the sixteen cosmids, only one, 153a8, showed specificity for the 5' end of the *mGluR8* cDNA while the others contained sequences from the middle of the cDNA or the 3' end.

FISH analysis of the 9 cosmids demonstrated that none spanned the

translocation breakpoint; all of the cosmids were localized proximal to the breakpoint with the exception of 153a8 (summarized in Table 4.1). This cosmid, specific for the 5' end of the cDNA and known to contain a CpG island (see previous chapter), was found to lie directly distal to the breakpoint (Figure 4.3). These results indicated that the *GRM8* gene was disrupted by UF53's translocation. Also, combined with previous mapping of the 3' end of *GRM8* to the centromeric end of HSC7E1289 and physical mapping of the region (Alley et al., 1996), my results indicated that the *GRM8* gene spans at least 700 kb in the genome.

PCR of Exons 1 and 2. To localize the site of the *GRM8* disruption, PCR amplification of individual exons from cosmid DNA established that exons 1 and 2 were contained within cosmids 153a8 and 85b12 respectively (Figure 4.4). These results confirmed the interruption of the *GRM8* gene and established that the translocation breakpoint was in intron 1. Based on the previous experiments which physically mapped these cosmids on the YAC contig (Alley et al., 1996), the intron was estimated to be at least 100 kb in size. Additionally, Southern blot analysis of the *GRM8* cosmids confirmed that exon 2 was contained in 85b12 as well as four other cosmids (15a5, 85b12, 41e10, and 41h9). These four cosmids, which had previously mapped to the same location in the 7q32 contig (Figure 3.5), were confirmed to overlap 85b12.

Discussion

GRM8 was one of two members of the gene family encoding the metabotropic glutamate receptors which had been mapped to human chromosome 7; *GRM3* had mapped to the 7q21.1-7q21.2 region (Scherer et al., 1996). Originally, a partial cDNA of *GRM8* was mapped to the centromeric end of the YAC HSC7E1289 (Scherer et al., 1996) that spans the UF53 breakpoint

Table 4.1 Summary of FISH Experiments with *GRM8* Cosmids

<u>Cosmid clones</u>	<u>Location relative to the translocation breakpoint</u>
13e6	proximal
15a5	proximal
41e10	proximal
85b12	proximal
109c4	proximal
150h8	proximal
153a8	distal
153f7	proximal
192d4	proximal

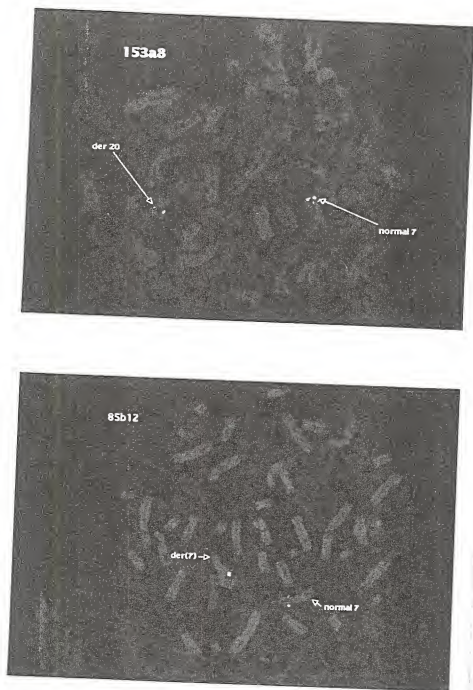


Figure 4.3. FISH analysis of the UF53 translocation region using cosmid clones containing the *GRM8* coding sequence. Digoxigenin-labeled cosmids (pink) were hybridized to metaphase chromosomes under competition with human Cot-1. UF53 metaphase spreads after hybridization with the cosmid clones (a) 153a8 and (b) 85b12 demonstrated distal and proximal positioning of probes, respectively. Chromosomes were counterstained with DAPI.

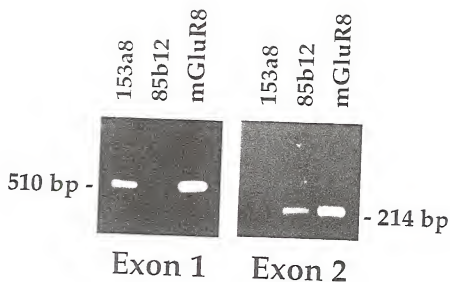


Figure 4.4. PCR amplification of *GRM8* exons 1 and 2. Cosmid clones 153a8 and 85b12 and the full-length *mGluR8* cDNA were tested for the presence of exon 1 (left-side panel) or exon 2 (right-side panel) by PCR amplification. PCR primers were specific for the 5' and the 3' ends of exons 1 and 2. The sizes of the products are indicated at the side of each panel.

(Alley et al., 1995). With my subsequent experiments, I demonstrated that *GRM8* is directly interrupted by UF53's translocation and that the breakpoint lies within intron 1. To fit the autosomal recessive inheritance of SLOS and provide further evidence for *GRM8* as an SLOS candidate gene, demonstration of a mutation in the other UF53 *GRM8* allele would have been required. However, mutational analysis of individual exons was not feasible at the time since the gene structure had not been fully elucidated, and mRNA from appropriate tissue (brain and retina) was not available for mutation screening since UF53 was deceased and only skin fibroblasts and lymphoblasts were available.

The CpG island I discovered in HSC7E1289 and the cosmid 153a8 corresponds to the 5' end of *GRM8*. Physical mapping of *GRM8* suggests that the genomic size of this gene is 700-1300 kb. Figure 4.5 illustrates the relative position and orientation of the *GRM8* gene with respect to HSC7E1289. Preliminary data suggests that the *GRM8* transcript is approximately 2.7 kb in size, indicating that the vast majority of the genomic sequence is represented by the introns (Dr. Stephen Scherer, personal communication). Intron 1 is estimated to be at least 100 kb in length, and therefore the interval containing the translocation breakpoint location remains quite large. Because there is no known connection between the glutamate receptor and cholesterol biosynthesis, and further mutational studies in UF53 are not yet possible, the role of *GRM8* in SLOS, if any, is not clear. I propose several hypotheses about the involvement of *GRM8* in SLOS. First, *GRM8* may be the affected *SLOS* gene in our patient through a biochemical mechanism not yet understood, with a mutation existing on the other allele. Since genetic heterogeneity might play a role in SLOS, *GRM8* may or may not be the affected gene in other SLOS families. Secondly, due to the large size of the intron 1, one could speculate that there are other functional genes embedded within this *GRM8* intron, as seen in *NF1* and the choline

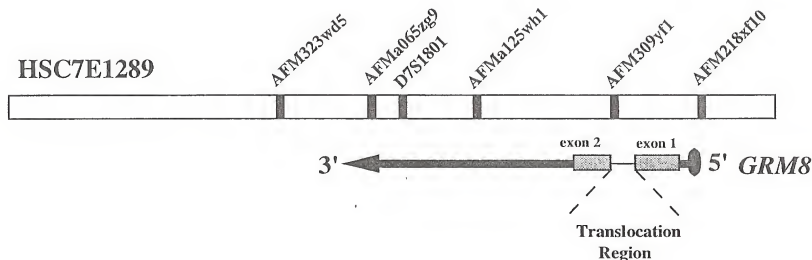


Figure 4.5. Illustration of the relative position and orientation of the *GRM8* gene on YAC HSC7E1289. Exons 1 and 2 were positioned based on experiments which placed 153a8 and 85b12 distal and proximal, respectively, to the DNA marker AFM309yf1. The sizes of the untranslated 5' and 3' ends and sizes of the introns are not known. The estimated minimal distance between AFM218xf10 and AFMa065zg9 is 700 kb, with maximal size estimated at 1,100 kb, based on PFGE and YAC overlap data.

transferase gene (Bejanin et al., 1994; Cawthon et al., 1990); one of these could be the actual *SLOS* gene functionally disrupted by the translocation. Third, it is possible that *GRM8* is not involved in *SLOS* and was coincidentally interrupted by the translocation in UF53. Forth, UF53 may have *SLOS* due to mutations at another locus, with no mutation on the other *GRM8* allele. However, part of her clinical picture may be attributed to her being functionally hemizygous at *GRM8* - the effect of this genotype is unknown. Further analysis of UF53 and other *SLOS* patients will be necessary to test each of these hypotheses.

Of additional interest is the linkage of an autosomal dominant form of retinitis pigmentosa (RP) to the 7q32 region. RP collectively refers to a group of degenerative retinal disorders that affect the photoreceptors and retinal pigment epithelium, resulting in night blindness and loss of peripheral vision of early adulthood (Heckenlively et al., 1988). RP is a genetically heterogeneous disease with forms including autosomal dominant, autosomal recessive, and X-linked modes of inheritance (Humphries, 1993). The autosomal dominant form had been associated with eight different loci including the *RP10* locus linked to 7q in two large unrelated RP families (Jordan et al., 1993; McGuire et al., 1995). The linkage data from the two families established that the *RP10* gene was flanked by the markers D7S686 and D7S530 which are separated by 5 cM (McGuire et al., 1996). These two markers were mapped on a 5 Mb interval in a large YAC contig, containing the 7q32 *SLOS* YAC contig. The highest combined lod score, 13.08, was associated with marker D7S514. This is the same marker flanked by the two *GRM8* cosmids, 153a8 and 85b12, which flank the translocation. *GRM8* seems a particularly interesting candidate gene for RP10 based on its reported expression in the retina of adult mice (Duvoisin et al., 1995). I propose that one theory is that a defect in *GRM8* is responsible for both RP10 and *SLOS*. Although there are no reports of *SLOS* patients with RP, it is interesting to speculate that

the loss of a single *GRM8* allele results in RP10, an autosomal dominant disorder, while the loss of both *GRM8* alleles results in SLOS, an autosomal recessive disorder. Given that many SLOS patients do not live beyond early childhood and therefore would not develop RP (regardless of gene mutations), this theory and the role of *GRM8* in RP10 and SLOS merits further investigation.

CHAPTER 5 MICROSATELLITE TYPING AND SOUTHERN BLOT ANALYSIS

Introduction

The interruption of *GRM8* by UF53's translocation is the first discovery of a gene disrupted in an SLOS patient. Unfortunately, without the full *GRM8* gene structure, it is impossible to test the other allele in UF53 for mutations. To further investigate the possible relationship between *GRM8* and SLOS, microsatellite genotyping was performed on a large SLOS family with microsatellite markers in the 7q32 region. In addition, to try to more closely map the translocation breakpoint, probes from exon 1 and 2 were designed for Southern blot analysis of UF53's genomic DNA.

Microsatellite Genotyping. The variable expression seen in both the clinical and biochemical presentation of SLOS suggests genetic heterogeneity. Genetic heterogeneity refers to the notion that different mutations can cause similar phenotypes. Genetic heterogeneity is subdivided into allelic heterogeneity (different mutations at the same locus) and locus heterogeneity (mutations at different loci). Several reports support the theory of locus heterogeneity in SLOS. Berry et al. reported a family with both SLOS and Miller-Dieker syndrome segregating independently; no cholesterol findings were reported (Berry et al., 1989). The children all carried unbalanced karyotypes which arose from meiosis of one parent's balanced translocation [t(7;17)(q34;p13.1)], implying that an *SLOS* locus may lie in the 7q34-qter region or in the 17p13.1-pter region. An individual with severe SLOS features, low

serum cholesterol, and normal concentrations of 7-DHC, was reported with an interstitial deletion at 17p13 related to a balanced paracentric inversion in the father [inv(17)(p11.2p13)], implicating proximal chromosome 17p in non-typical SLOS (Yang et al., 1994). Additionally, there was a report of three sisters having SLOS-like features with a small terminal deletion of chromosome 4 (Hill et al., 1991). Although these patients did not have the classic SLOS clinical and/or biochemical phenotype (in some cases the tests were not done), is it possible that recessive mutations at several genetic loci can independently result in SLOS?

To address the question of heterogeneity, I chose to genotype the microsatellite markers in the 7q32 translocation region to determine if there was any co-inheritance between the loci and SLOS in other families. SLOS families with one or more affected siblings were collected through various clinical collaborations. The most extensive SLOS family (Figure 5.4), consisting of multiple affected siblings as well as affected first cousins, was provided by Dr. Ngozi Nwokoro (Cleft Palate - Craniofacial Center, University of Pittsburgh). Microsatellite analysis had two possible outcomes: 1. identical genotypes among affected siblings with no unaffected siblings having the same genotype, thus indicating consistent inheritance of SLOS and this region, or 2. a variation of the above rules, thereby ruling out that the *SLOS* locus in that family resides with the *GRM8* region. If all of the markers were consistent with an *SLOS* locus in that region, further investigation, such as *GRM8* mutational analysis, would be warranted in these families.

Microsatellites are defined as a group of short tandemly repeated sequences that are found throughout the human genome (Hughes, 1993). Commonly, microsatellite repeats are composed of the dinucleotide (CA)_n, which is particularly abundant in the human genome. It is estimated that as many as 50,000 microsatellites are found throughout the genome with the unit of

repeat containing from 10-60 copies of the dinucleotide sequence (Jeffreys et al., 1990; Weber and May, 1989). These highly polymorphic repeats serve as extremely useful markers for the mapping of disease genes and overall genetic mapping of the genome. Microsatellite markers are typed by amplification of the repeat unit using PCR primers specific for the microsatellite of interest, and analysis of the PCR products on a denaturing polyacrylamide sequencing gel as illustrated in Figure 5.1.

Southern blot analysis. Since the translocation lay in such a large intron, I could not rule out disruption of an embedded gene other than *GRM8* as the SLOS associated event. Localization of the breakpoint in close proximity to either exon 1 or 2 would lend more support for *GRM8*'s role than an internal gene. In an attempt to detect the translocation by Southern blot analysis, I generated PCR fragments from exons 1 and 2 to use as probes against Southern blots of UF53 genomic DNA. Repeated failure of these small probes to hybridize led to my characterization of additional sequence outside of the open reading frame by direct sequencing of cosmids. Sequencing directly from cosmids is a challenging task since success is dependent upon the integrity of the large cosmid DNA molecule. To insure that the cosmid DNA was greater than 85% supercoiled, I purified the DNA with the Nucleobond™ AX 500 Kit (Macherey-Nagel). I designed internal sequencing primers from exon 1 and 2 which would allow for the generation of sequence 5' to each of the exons. I obtained approximately 300 additional bp of sequence in the 5' untranslated region of exon 1, but no sequence was obtained 5' of exon 2 despite numerous attempts. From the new sequence in exon 1, I designed primers which amplify a 613 bp fragment containing 5' untranslated sequence and open reading frame (Figure 5.2). Unfortunately, hybridization of the 613 bp fragment against the UF53 Southern blot resulted in nonspecific repetitive hybridization which I could not eliminate

Microsatellite Typing

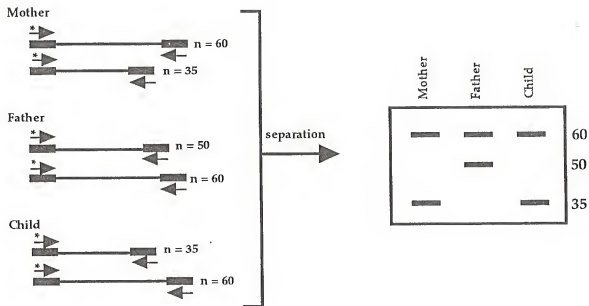


Figure 5.1. Schematic of microsatellite typing. Microsatellite analysis is performed using PCR primers specific for each microsatellite marker. One of the two primers (indicated by arrows on the left panel) is end-labeled with γ - ^{32}P dATP using kinase (indicated by the *). The patient's DNA is then subjected to PCR using these primers and the PCR products are separated on a 6% denaturing polyacrylamide gel. The genotype of each individual can then be determined from autoradiography of the gel (right-side panel). In the example illustrated here, the mother has one allele with 60 repeats and the other with 35 repeats, while the father has alleles of 50 and 60 repeats. Thus, the child inherited the allele with 35 repeats from the mother and the allele with 60 repeats from the father.

5'-caggaatat tctgctacaaggctgatttcaaggacatgaattgttgacc
tcatcccaacatcagaacct, cagatgttctaatttttgaccattccaggca
 agttgatcttataaggaaataaaattgaaccttaggggtctgatggaaatt
 cactgtgacattcaaatcaagaaaacttgctaatgcccaagagccttttcc
 ccatgggcccctgatggtagcctccagaagggtgcagcctcagggtgggtgcc
 ttcttctgttggaagaataaaactttgggtcttggattgcaataccacctgt
 ggagaaa ATGGTATGCGAGGGAAAGCGATCAGCCTCTT
 GCCCTTGTTCCTCCTTGACCGCCAAGTTCTACTGG
 ATCCTCACAATGATGCAAAGAACTCACAGCCAGAGTA
 TGCCCATTCATACGGGTGGATGGGGA CATTATTTTG
 GGGGGTCTCTTCCTGTCCACGCAAAGGGAGAGAGAG
 GGGTGCCTTGTGGGGAG*CTGAAGAAGGAAAAGGGAT
 TCACAGACTGGAGGCCATGCTTTATGCAATTGACCAG
 TTAACAAGGCCCTGTCTCCTTTTCCAACATCACTCTGG
 GTGTCCGCATCCTCGACACGTGCTTCTAGGGACACC **AT**
ATGCTTTGGAGCAGTCACTAAC AATCGTGCAGGCATT
 AATAGAGAAAGATGCTTCGGATGTGAAGTGTGCTAAT
 GGAGATCCACCCATTATTACCAAGCCCGACAAGATT
 TCTGGCGTCATAGGTGCTGCAGCAAGCTCGTGTCCAT
 CATGGTT GCTAACAT TTTAAGACTTTTTAAGATAC-3'

Figure 5.2. Partial nucleotide sequence of *GRM8* exon 1. The 5' untranslated region and open reading frame are shown in lower-case and upper-case, respectively. PCR primers were designed from the underlined sequence (arrows indicate orientation). The translational start site, ATG, is italicized and the *AluI* restriction site is shown in bold type with the asterisk representing the cleavage site.

with Cot-1 competition. I searched the sequence for restriction sites to generate smaller fragments that might have a less repetitive nature. An AluI restriction site was located toward the 3' end of the fragment, which produced two fragments of 460 bp and 153 bp in size (Figure 5.2). The 460 bp fragment successfully hybridized against the Southern blot of UF53, and no gross DNA abnormalities were detected.

Materials and Methods

Isolation of genomic DNA from patient leukocytes or fibroblasts. Patient blood or fibroblast cell line samples were acquired from the following clinicians: Dr. Mira Irons (New England Medical Center, Boston), Dr. Ngozi Nwokoro (Cleft Palate - Craniofacial Center, University of Pittsburgh), Dr. Laura Keppen (University of South Dakota School of Medicine, Sioux Falls), Dr. Richard Kelley (Kennedy Krieger Institute, Baltimore) and Dr. Dianne Abuelo (Rhode Island Hospital, Providence). DNA was isolated from the leukocytes following basic procedures as follows (Madisen et al., 1987). Whole blood samples were separated by centrifugation in EDTA vacutainer tubes at 3000 rpm for 10 minutes. The buffy coat containing the leukocytes was transferred to a sterile 50 cc conical tube. Forty-five ml of RBC lysis solution (0.15 M ammonium chloride, 0.02 M Tris, pH 7.65) was added, mixed, and incubated at 37°C for several minutes to lyse red blood cells. Leukocytes were pelleted by centrifugation at 2000 rpm for 5 minutes. The supernatant was poured off and the pellet gently washed with 1XPBS (phosphate-buffered saline). The pellet was resuspended in 5 ml high TE (100 mM Tris, pH 8.0; 40 mM EDTA, pH 8.0) and 5 ml Lysis Solution (high TE with 0.2% SDS) were added to lyse the leukocytes. The DNA was phenol/chloroform extracted, isopropanol precipitated, and resuspended in approximately 1 ml of TE. DNA concentrations were determined by

fluorometry. For fibroblasts, these were grown in culture under our standard conditions (Alley et al., 1995) and the cells harvested by trypsinization. The cells were washed in PBS and lysed as the leukocytes above, with the rest of the procedure being the same.

Microsatellite genotyping of patient samples. Three microsatellite markers (AFM218xf10, AFM309fy1, and AFMa125wh1) from the translocation region were used to study the SLOS families. One primer of each set was end-labeled with γ -³²P dATP using T4 polynucleotide kinase (Sambrook et al., 1989). The PCR reactions were performed with 25-50 ng genomic DNA, 200 mM of each dNTP, 40 ng of cold primer (forward and reverse), 6 ng of end-labeled primer, 1.0 units of *Taq* polymerase, using standard buffer conditions in a total volume of 20 μ l. PCR was performed using a Perkin Elmer Cetus 480 thermal cycler with the following conditions: 2 minutes hot start at 94°C, then 30 cycles of 94°C for 40 seconds, 62°C for 40 seconds, and 72°C for 40 seconds followed by an extension at 72°C for 5 minutes. A 10 μ l sample of each reaction plus 10 μ l of stop buffer was heat denatured and electrophoresed on a 6% denaturing polyacrylamide gel. The bands were visualized by autoradiography.

Sequence of 5' untranslated region of exon 1. Cosmid 153a8 was grown as previously described and the DNA purified according to the protocol for the Nucleobond™ AX 500 Kit (Macherey-Nagel) to insure that greater than 85% of the recovered DNA was in its supercoiled configuration. One μ g of 153a8 cosmid DNA was prepared for sequence analysis according to the protocol for the *Taq* DyeDeoxy™ Terminator Cycle Sequencing Kit (Applied Biosystems). The sequencing primer (5'-TGCATCATTGTGAGGATCCAGTAG-3') was designed from internal sequence in the open reading frame of exon 1. The samples were then subjected to cycle sequencing using the Perkin Elmer Cetus model 480 thermal cycler with the following conditions: hot start at 96°C followed by 25

cycles of 30 seconds at 96°C, 15 seconds at 50°C, and 4 minutes at 60°C. The sequencing reactions were ethanol precipitated, dried, and the DNA resuspended. Sequence was analyzed on the ABI Automated Sequencer 373A through the Center for Mammalian Genetics.

Southern blot analysis of UF53. A 613 bp genomic fragment from GRM8 exon 1 was amplified from cosmid 153a8 using the above conditions. The primers used were (5'-TCATCCCAACATCAGAACCT-3'), in the 5' untranslated region, and (5'-GTTAGTGACTGCTCCAAAGCATA-3'), in the open reading frame (Figure 5.2). The 613 bp product, containing 278 bp of the 5' untranslated region, was then subjected to digestion with the restriction endonuclease AluI, to produce a 460 bp and 153 bp fragment. The 460 bp fragment (the 5' end) was purified according to the QiaQuick protocol (Qiagen,) and labeled by random-priming with alpha-³²P dCTP (Mega Prime kit, Amersham). For the Southern blot analysis, UF53's DNA was independently digested with the restriction enzymes EcoRI, HindIII, and PstI, subjected to agarose gel electrophoresis, transferred to Hybond N (Amersham), and hybridized as previously described (Wallace et al., 1990). The wash conditions were based the Church and Gilbert SDS/sodium phosphate method at 60°C (Church and Gilbert, 1984). Signals were detected with autoradiography.

Results

Microsatellite genotyping. To demonstrate coinheritance of SLOS and the 7q32 markers in an SLOS family, affected siblings would have to display identical genotypes while unaffected siblings must have genotypes unlike their affected siblings. The results of the microsatellite genotyping revealed that the Nwokoro family was inconsistent for coinheritance of the 7q32 markers and SLOS (Figure 5.3 and 5.4). UF339, affected, and UF448, unaffected, are sisters in

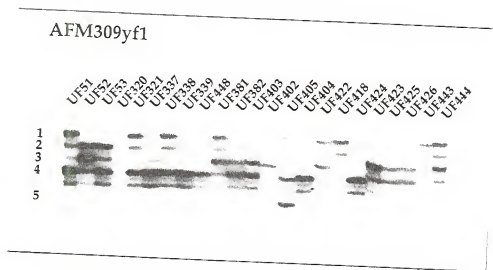


Figure 5.3. Autoradiograph of microsatellite typing of AFM309yf1 in the SLOS patients/family members. The numbers indicate the arbitrary allele name assignments (exact sizes undetermined).

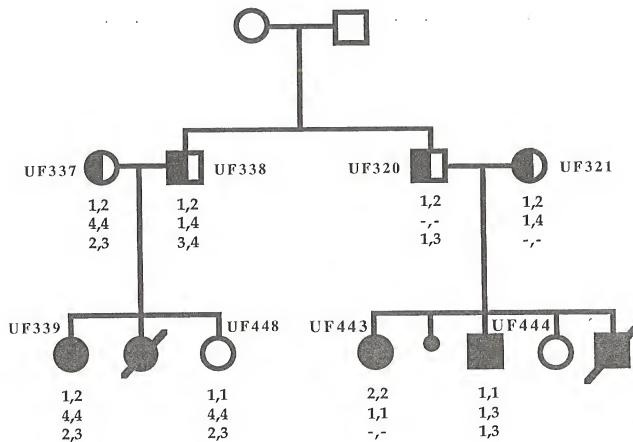


Figure 5.4. Pedigree of SLOS family from Dr. Ngozi Nwokoro. DNA has been obtained from individuals with UF numbers. Half-shaded symbols represent obligate carriers, fully-shaded symbols represent affected individuals. Genotypes determined by microsatellite typing of AFMa125wh1, AFM309yf1, and AFM218fx10 are shown below each individual. It is unknown which individual in the top generation was the carrier.

the same nuclear family displaying the same genotypes for the markers AFM309yf1 and AFM218xf10. Also, UF443 and UF444, who are both affected and are first cousins to UF339 and UF448, display different genotypes for the markers AFMa125wh1 and AFM309yf1. This clearly rules out the *GRM8* region as having the Nwokoro family *SLOS* gene, with virtual certainty.

Southern blot analysis. Southern blot analysis of UF53 was performed using a genomic probe derived from exon 1 to determine if the translocation breakpoint lay near exon 1, and to assay for any additional gross DNA rearrangements. The 460 bp probe detected 8-10 kb *EcoRI* and *HindIII* fragments and a 6.0 kb *PstI* fragment (Figure 5.5). No abnormalities in band size or intensity were apparent with *EcoRI* and *HindIII*. Although the UF53 *PstI* band appears to be less intense than the control, ethidium bromide staining of the gel revealed that this lane was under-loaded with respect to the control (data not shown). Therefore, the results suggest that the breakpoint does not lie within the vicinity of exon 1 and no obvious rearrangements lie in this region on the other allele.

Discussion

Microsatellite genotyping. Microsatellite genotyping of the three markers, AFMa125wh1, AFM309yf1, and AFM218xf10 was extended to all patient samples including the Nwokoro family, UF53 and parents, and various relatives and patients of other *SLOS* families (Figure 5.3). However, since most of the families were incomplete or I only had DNA from one child, there were no conclusive results from the genotyping except for the Nwokoro family. The genotyping of UF53's family, while not pertinent to this study, was important for future genetic studies since it showed that the genotypes were consistent with correct paternity. The microsatellite genotyping demonstrated that the Nwokoro family did not fit the model for coinheritance of *SLOS* and the 7q32 markers, and I can reasonably

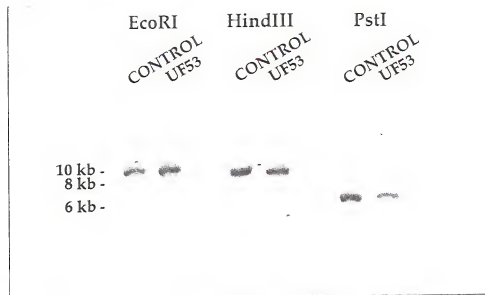


Figure 5.5. Autoradiograph of Southern blot analysis of EcoRI digests of UF53 and control DNA with 460 bp PCR fragment probe from *GRM8* exon 1. The sizes, indicated to the left, were estimated from a 1 kb molecular weight marker.

conclude that *GRM8* is not the *SLOS* gene in the Nwokoro family. If *GRM8* is ultimately confirmed as the *SLOS* gene in the UF53 family, the lack of association between *SLOS* in the Nwokoro family and the 7q32 locus would support the theory of genetic locus heterogeneity.

Southern blot analysis. Southern blot analysis with exon 1 did not show any abnormal banding patterns in UF53, ruling out rearrangements at the 5' end of intron 1. Therefore, the translocation region is still considerably large and further mapping of the intron would be necessary to determine its precise location. This would be pertinent to pursue the possibility of an embedded gene playing a role.

To determine if any of the rare-restriction sites contained within cosmid 153a8 were in the known sequence of exon 1 of *GRM8*, a computer search for BssHII, MluI, and NotI restriction sites in the sequence was conducted (Alley et al., 1996). The search yielded no rare-restriction sites for the endonucleases, suggesting that the CpG island is outside this region, most likely further upstream based on the CpG island literature.

CHAPTER 6

CONCLUSIONS AND FUTURE DIRECTIONS

Conclusions. The aim of my studies was to examine the UF53 translocation breakpoint region to determine if any genes were disrupted, thereby identifying potential candidate genes for SLOS. My work has lead to the identification of the first candidate *SLOS* gene disrupted at the molecular level.

As described in Chapter 2, using FISH analysis of YACs, I identified a 1,800 kb YAC, called HSC7E1289, that spans UF53's translocation breakpoint. The translocation, which was originally mapped to the cytogenetic band of 7q32.1, was resolved to a megabase level with the localization of this YAC. I further narrowed this region by FISH analysis of YACs known to overlap HSC7E1289. The results mapped HSC7E1351 and HSC7E244 proximal and distal to the translocation, respectively, placing the breakpoint tentatively between markers AFMa125wh1 and AFM309yf1. Although these markers are separated by approximately 200-300 kb, the translocation breakpoint could not be excluded from a larger region of HSC7E1289, since the probes generated from the YACs were fragments derived from *Alu*-PCR. The distribution and orientation of the *Alu* elements was not known for the YACs and the fragments may not have represented the entire YAC. Therefore, a conservative estimate of 1 Mb for the translocation breakpoint region was proposed.

In Chapter 3, I discussed the construction of a physical map of the YAC clones (HSC7E1289, HSC7E122, c752c8, HSC7E476, HSC7E261 and HSC7E244) surrounding the translocation breakpoint, by PFGE using restriction

endonucleases that recognized rare-restriction sites. The rare-restriction site mapping established the presence of two CpG islands in the contig. One CpG island was located on the telomeric end of HSC7E1289, and the other was approximately 500 kb distal. The latter CpG island was found to correspond to the *PAX4* gene, which had previously been mapped to the same region by Southern blot analysis of the YAC clones with a *PAX4* mouse cDNA clone. An intriguing aspect of *PAX4* is that this gene (and all other members of the *PAX* gene family) are monoallelically expressed in the absence of genomic imprinting (Dr. Shirley Tilghman, personal communication). It is possible, though perhaps unlikely that the translocation of the active *PAX4* allele resulted in the suppression of its expression.

In Chapters 3 and 4, a series of studies led to the conclusion that the *GRM8* gene was interrupted by the translocation in UF53. The mapping of a partial *GRM8* cDNA to the centromeric end of HSC7E1289 was the turning point in my positional cloning effort. Hybridization of the full-length *mGluR8* cDNA against Southern blots of the YAC clones revealed that the gene was distributed across the contig. YAC clones known to lie proximal and distal to the breakpoint, as well as HSC7E1289, had hybridization patterns which suggested that the *GRM8* gene was possibly interrupted by the translocation. The full-length *mGluR8* cDNA was also used to screen a human chromosome 7-specific cosmid library which resulted in the retrieval of 16 cosmids. These cosmids were localized along a 700 kb section of the contig by hybridization of unique sequences from each cosmid against YAC Southern blots. One cosmid, 153a8, was localized to the same region of the CpG island found in HSC7E1289, and was found to contain that CpG island. FISH analysis identified two cosmids, 153a8 and 85b12, which lie distal and proximal to the translocation, respectively. 153a8 was known to be specific for the 5' end of the *mGluR8* cDNA and contained a CpG island,

implying that the 5' end of the *GRM8* gene falls distal to the breakpoint. In order to localize the *GRM8* disruption, PCR amplification of individual exons from the cosmids 153a8 and 85b12 was performed. Exon 1 was found to be contained within 153a8 while exon 2 was identified in 85b12. These results confirmed the interruption of the *GRM8* gene and established that the breakpoint was in intron 1, which is estimated to be approximately 100 kb.

The translocation breakpoint could not be detected at the 5' end of intron 1 by Southern blot analysis as discussed in Chapter 5. Hybridization of a 460 bp exon 1 probe against a Southern blot of UF53 revealed no aberrations with the three restriction endonucleases.

Chapter 5 also addressed whether SLOS was genetically heterogeneous in nature. Three microsatellite markers from the 7q32 region, (AFMa125wh1, AFM309yf1, and AFM218xf10) were genotyped in SLOS families including the large Nwokoro family, UF53's family, and various relatives and patients of other SLOS families. Due to the lack of complete families, conclusive results were obtained only from the Nwokoro family. Microsatellite genotyping of this family showed that with a high probability, the aforementioned markers and SLOS were not coinheritied based on the genotypes of affected and unaffected siblings. In order to fit the model of an *SLOS* gene lying in the *GRM8* region, affected individuals would have to share the same genotype while unaffected siblings would have genotypes distinct from their affected siblings. This was not the case in the Nwokoro family, indicating that the *SLOS* locus in this family is elsewhere in the genome. The elimination of the Nwokoro family's *SLOS* locus from the 7q32 region implies there are most likely at least two loci involved in SLOS, assuming that UF53's *SLOS* locus is *GRM8* or another gene in the region. Locus heterogeneity in SLOS is also plausible since it is logical that defects in other enzymes/proteins of the cholesterol pathway besides 7-DHCR could lead to

cholesterol and/or 7-DHC level abnormalities. Recently, Dr. Kelley from the Kennedy Krieger Institute contacted us about a mildly affected SLOS patient having "a defect of sterol transport rather than biosynthesis", determined by radioactive tracer studies (Dr. Richard Kelley, personal communication). The patient had a cholesterol profile indistinguishable from other SLOS patients, supporting the notion that a different genetic defects can cause SLOS.

Future directions. I had put forth the hypothesis that UF53's translocation breakpoint, at the 7q32.1 region, directly disrupts one allele of a putative *SLOS* gene while a more subtle mutation disrupts the other allele. However, without the *GRM8* genomic sequence, I was unable to determine if another mutation interrupted the other *GRM8* allele. I feel that once the entire cDNA sequence and exon structure is made available, mutational analysis of the other allele is essential. Heteroduplex analysis and single-strand conformation polymorphism (SSCP) analysis can be used in concert to screen for mutations found in or around the *GRM8* exons. Heteroduplex and SSCP analysis are both PCR based tests which can detect subtle mutations, such as base substitutions and small insertions or deletions, demonstrated by aberrant migration on polyacrylamide gels relative to controls (Hayashi and Yandell, 1993).

Heteroduplex analysis begins with PCR amplification of the region of interest (White et al., 1992). The PCR products, containing both alleles, are denatured by heat and then slowly reannealed. The DNA will reanneal, forming perfectly matched duplex DNA fragments (homoduplexes) and duplex DNA fragments in which the strands differ slightly, called heteroduplexes, if the two alleles differ. The heteroduplex is a result of a base substitution, an insertion or a deletion on one allele relative to the other. The detection of the heteroduplex is based on abnormal migration on a native polyacrylamide gel with respect to the normal homoduplexes.

SSCP analysis, like heteroduplex analysis, begins with the PCR amplification of the region of interest such as an exon (Hayashi and Yandell, 1993). The PCR products are heated to produce single strands to be separated on a non-denaturing polyacrylamide gel. The single strands of DNA will fold upon themselves in a unique confirmation determined by their primary sequence under the non-denaturing conditions. The presence of a mutation often alters the migration of the single-stranded product. If heteroduplex and SSCP analysis do not detect any mutations in UF53's DNA, the ultimate strategy would be to sequence all of the exons. If a mutation in UF53's other *GRM8* allele was still not detected it would cease to be a candidate gene for SLOS. Since SLOS is an autosomal recessive disorder, both alleles of any putative *SLOS* gene would have to be disrupted in such a way that the function of the encoded protein would be predicted to be altered in some fashion.

If *GRM8* is eliminated as a candidate gene for SLOS in UF53, based on the failure to identify another mutation in the other allele, I feel the next logical step in ruling out the region would be to search intron 1 for embedded genes. As I had eluded in Chapter 4, it is plausible that a gene is embedded within the 100-kilobase intron 1, whose disruption results in SLOS. A methodology well suited for this search is exon trapping, an established technique which recovers exons in a genomic region (Church et al., 1994; Niu and Crouse, 1993). In exon trapping, target genomic DNA is shotgun subcloned into an exon trap vector (i.e. pSPL3) having a multiple cloning site flanked by functional splice donor and acceptor sites. The recombinant plasmids are transfected into COS-7 (monkey kidney) cells where splicing will occur if the cloned DNA contains an exon in the proper orientation. The RNA produced by the splicing event is extracted and used for synthesis of first strand cDNA which is then amplified using primers complementary to the splicing vector. The recovered PCR products are cloned

and analyzed for inserts that represent putative exons. Due to the large size of the *GRM8* intron 1, several cosmids representing the region would have to be used for exon trapping to maximize the chance that all possible genes embedded in the intron would be recovered (Monaco, 1994). Alternatively, P-1 derived artificial chromosomes (PACs), which have sizes of approximately 100 kb, could be used for exon trapping if one or more is found to contain intron 1. A distinct disadvantage of exon trapping is the failure to detect intronless or single intron genes (Monaco, 1994). Therefore if exon trapping fails to detect any exons, cDNA direct selection could be pursued to further screen the intron (discussed in Chapter 3).

Another approach to studying the involvement of *GRM8*, or other candidate *SLOS* genes, in SLOS would be the creation of a knockout mouse for the candidate gene (Joyner, 1993). Briefly, a mutation in the candidate gene (usually a major disruption via insertion) is introduced in a mouse embryonic stem (ES) cell line by homologous recombination. The mutation is selected and confirmed, and the mutation-bearing ES cells are injected into blastocysts and implanted into pseudo-pregnant mice. Progeny are mosaic and are bred to create a line of fully heterozygous mice (one normal and one mutant allele). These mice can then be crossed to produce homozygous mutant pups, whose phenotype would be compared to SLOS. If the knockout gene is involved in SLOS, one would expect that knockout homozygotes would produce a phenotype similar to that of SLOS and/or display early lethality. This is one way to functionally analyze a candidate gene, although, since knockout mouse lines do not always produce the expected phenotype, this method may not yield useful data. However, if the mouse phenotype recapitulated SLOS, it would provide a model for understanding development of SLOS features throughout

embryogenesis, and would provide a model for testing genetic or medical therapies.

In addition to the continued investigation of *GRM8* and its relation to SLOS, I feel it is imperative to examine other genes which may also be potentially involved in the disorder. As I mentioned in Chapter 5, SLOS is believed to be genetically heterogeneous, implying that more than one gene may be responsible for the SLOS phenotype. Literature review revealed several interesting genes involved in the regulation of cholesterol synthesis and cholesterol transport. These include the genes for sterol regulatory element binding proteins 1 and 2 (SREBP-1 and -2) and sonic hedgehog (SHH).

SREBP-1 and SREBP-2, the protein products of the *SREBF-1* and *SREBF-2* genes, are structurally related proteins involved in the regulation of cholesterol homeostasis (Hua et al., 1993; Wang et al., 1993). SREBP-1 and SREBP-2 bind to the sterol regulatory element-1 (SRE-1) in the promoters of the low density lipoprotein receptor gene (Yokoyama et al., 1993) and the 3-hydroxy-3-methylglutaryl CoA (HMG-CoA) synthase, HMG-CoA reductase, and farnesyl diphosphate synthase genes (Ericsson et al., 1996; Vallett et al., 1996; Wang et al., 1993), activating transcription. Additionally, the SREBPs activate several of the genes involved in fatty acid biosynthesis (Hua et al., 1996).

The SREBPs have a tripartite structure consisting of an NH₂-terminal segment (the transcription factor), a middle segment composed of two membrane spanning regions separated by a hydrophilic domain, and a carboxy-terminal segment (Hua et al., 1996). Both proteins are bound to the endoplasmic reticulum and nuclear envelope, with their NH₂-terminal and carboxy-terminal segments projecting into the cytosol (Hua et al., 1995). In the absence of cholesterol and other sterols, a two step proteolytic process releases the NH₂-terminal segment which enters the nucleus and activates transcription of the

aforementioned genes (Sakai et al., 1996). The first cleavage, resulting in the cleavage of the hydrophilic domain between the transmembrane spanning regions, is dependent upon sterol concentrations. The second cleavage is not sterol dependent and is responsible for the release of the NH₂-terminal segment containing the transcription factor. Recently, a SREBP cleavage activating protein (SCAP), responsible for regulation of cholesterol biosynthesis by stimulating the first cleavage step of SREBP-1 and -2, was isolated (Hua et al., 1996). SCAP, whose activity is sterol dependent, is hypothesized to regulate the protease which is involved in the first cleavage of the SREBPs by direct protein-protein interaction.

SREBF-1 and *SREBF-2* have been localized to chromosomes 17p11.2 and 22q13, respectively (Hua et al., 1995). Although neither of the *SREBFs* map to a region which has been implicated in SLOS, they are particularly interesting genes based on their extensive involvement in cholesterol and fatty acid synthesis. Based on the known biochemistry, it feasible that homozygous disruption of either gene could result in decreased serum and tissue cholesterol levels. Since the locations of both SREBP genes are known, microsatellite genotyping of our SLOS families with markers in and around these genes is feasible. Furthermore, sequences of the intron/exon boundaries of the *SREBF-1* gene are available which would allow mutational analysis in SLOS patients (Hua et al., 1995). Since the location and cDNA sequence of *SCAP* have not been elucidated, investigation of its involvement with SLOS is not yet possible.

SHH, unlike the SREBPs, has a more direct link to SLOS. The *SHH* gene encodes a secreted protein responsible for early embryo patterning in the vertebrate CNS, anterior-posterior limb axis and somites (Echelard et al., 1993; Fan and Tessier Lavigne, 1994; Riddle et al., 1993). Hh, the SHH homolog in *Drosophila*, undergoes autocatalytic processing mediated by its carboxy-terminal

domain, producing a lipid modified amino-terminal fragment (Echelard et al., 1993; Fan and Tessier Lavigne, 1994; Porter et al., 1996; Riddle et al., 1993). The modified amino-terminal fragment, responsible for signaling activity for embryonic patterning, was found to be covalently attached to cholesterol (Porter et al., 1996). The covalent modification with cholesterol appears to be essential for regional localization and concentration of Hh in various organizing centers in the developing *Drosophila* embryo (Porter et al., 1996).

SHH was recently identified as a gene for holoprosencephaly (HPE), a genetically and phenotypically heterogeneous malformation sequence involving the forebrain and midface (Belloni et al., 1996). HPE has been assigned to four distinct loci based on linkage and the analysis of chromosomal rearrangements in HPE patients (Gurrieri et al., 1993). Both *SHH* and HPE were mapped to the 7q36 region (Belloni et al., 1995; Belloni et al., 1996). Mutations in *SHH* were identified in patients with autosomal dominantly inherited HPE, indicating that the absence of one *SHH* allele is sufficient to produce the HPE phenotype (Roessler et al., 1996).

A casual connection between SLOS and HPE was made in 1991 when Verloes et al. described a group of patients with HPE and polydactyly that had other features resembling SLOS. Recently, four patients with clinically and biochemically confirmed SLOS and malformations characteristic of the HPE sequence were reported (Kelley et al., 1996). SLOS features included syndactyly of toes 2-3, micrognathia, mental retardation, cleft palate, and ambiguous genitalia. The incomplete HPE sequence was estimated to occur in the SLOS population at a frequency of 4% (Kelley et al., 1996). Thus, there can be clinical overlap between SLOS and HPE raising the question of genetic overlap. Another possible connection between these two disorders is based on the defect in cholesterol metabolism in SLOS and the improper signaling of the *SHH* gene in

HPE. *SHH* is also interesting since it resides at 7q36, a region suggested to be involved in SLOS based on the patient who was monosomic at 7q34-qter due to unbalanced translocation segregation (Berry et al., 1989). Kelley et al. (1996) proposed two mechanisms in which the defect in cholesterol metabolism in SLOS individuals might affect the function of the SHH protein. First, a deficiency in cholesterol could lead to inefficient processing of the SHH protein resulting in deficient signaling. Second, competition between 7-DHC and cholesterol for covalent linkage to the NH₂-terminal SHH fragment may result in an increased amount of 7-DHC-modified SHH protein which could subsequently result in inefficient or absent signaling. These two theories suggest that abnormal processing of SHH may be secondary to the abnormal cholesterol metabolism seen in SLOS patients, resulting in HPE features as well. Alternatively, I propose that *SHH* could be an *SLOS* gene. Inefficient SHH signaling due to certain mutations on both *SHH* alleles (possibly preventing binding to cholesterol) could lead to improper sterol metabolism. However, this theory assumes that some *SHH* mutations do not result in HPE, and that having mutations on both alleles is not necessarily a lethal condition. Mutational analysis of the *SHH* gene in our SLOS patient panel is currently underway.

Once an *SLOS* gene has been found and confirmed to contain mutations in SLOS patients, several issues can be addressed such as genetic heterogeneity, genotype/phenotype relationship, gene expression and regulation and general protein function. In order to efficiently test SLOS patients for mutations in *SLOS* gene(s), good mutational screening methods must be developed. The genomic structure of the gene will ultimately determine which strategies which will provide the most reliable and efficient mutation screening of the gene. The presence or absence of mutations in an *SLOS* gene would be the best evidence for or against genetic heterogeneity. If different loci were identified with mutations

in different SLOS patients, locus heterogeneity would be confirmed. Predictions about the effect of different mutations on protein function and how these lead to the clinical and biochemical profile seen in SLOS would also begin with mutational analysis. These data could in turn be used to develop pharmaceutical or other interventions early in embryogenesis.

Mutational analysis would also benefit known SLOS families by allowing prenatal diagnosis at the earliest possible stage (8-9 weeks via CVS) or even preimplantation. Genetic screening would be more powerful than the current biochemical screening since the biochemical analysis is not always consistent in SLOS and could be inaccurate due to maternal contamination of a fetal sample. Also it is unclear if carriers can always be biochemically distinguished from affected individuals at that stage in development. Early identification might be crucial if any therapies are developed since the defects begin early in embryogenesis.

The discovery of different mutations may eventually allow a correlation between genotype and phenotype to be made. Several questions can be addressed based on such studies. Do missense and in-frame mutations cause result in mild SLOS cases? Do nonsense and frameshift mutations and major disruptions cause severe SLOS? What is the phenotype of a person who has both a "mild" and a "severe" allele?

Elucidation of an *SLOS* gene will warrant studies addressing expression and regulation of the gene to build a sufficient foundation of knowledge to better understand its protein's normal function and pathogenesis of SLOS when it is defective. Protein studies will also contribute to the basic understanding of the functional or enzymatic activities of the gene product and their action of other genes and/or proteins.

I would like to conclude with a quote from Drs. Opitz and de la Cruz (1994) in which the clinicians and researchers involved in SLOS "agreed unanimously that research in this field be given highest priority in order to better understand cholesterol synthesis in the mammalian brain, cholesterol transport from mother to embryo to fetus, pre- and postnatal metabolic compensation in cholesterol synthesis, the nature of the blood-brain barrier for cholesterol, treatment of affected infants, children and adults, structure and genetic specification of a 7-DHC reductase enzyme (which has never been purified!) and its evolution, the variability of the syndrome and whether it is genetically homo- and heterogeneous, the population genetics of the RSH syndrome, possible selective advantages (or disadvantages) of heterozygotes, and means of newborn screening, carrier detection, and prenatal diagnosis."

REFERENCES

- Abe, T., Sugihara, H., Nawa, H., Shigemoto, R., Mizuno, N., and Nakanishi, S. (1992). Molecular characterization of a novel metabotropic glutamate receptor mGluR5 coupled to inositol phosphate/Ca²⁺ signal transduction. *J. Biol. Chem.* 267, 13361-8.
- Acosta, P. B. (1995). Theoretical and practical aspects of dietary treatment of Smith-Lemli-Opitz syndrome. *Int. Pediatr.* 10, 37-40.
- Alley, T. L., Gray, B. A., Lee, S. H., Scherer, S. W., Tsui, L. C., Tint, G. S., Williams, C. A., Zori, R., and Wallace, M. R. (1995). Identification of a yeast artificial chromosome clone spanning a translocation breakpoint at 7q32.1 in a Smith-Lemli-Opitz syndrome patient. *Am. J. Hum. Genet.* 56, 1411-6.
- Alley, T. L., Scherer, S. W., Huzienga, J. J., Tsui, L.-C., and Wallace, M. R. (1996). Physical mapping of the chromosome 7 breakpoint region in an SLOS patient with t(7;20)(q32.1;q13.2). *Am. J. Med. Genet.* 68, 279-281.
- Batta, A. K., Salen, G., Tint, G. S., and Shefer, S. (1995). Identification of 19-nor-5,7,9(10)-cholestatrien-3 beta-ol in patients with Smith-Lemli-Opitz syndrome. *J. Lipid Res.* 36, 2413-8.
- Bejanin, S., Cervini, R., Mallet, J., and Berrard, S. (1994). A unique gene organization for two cholinergic markers, choline acetyltransferase and a putative vesicular transporter of acetylcholine. *J. Biol. Chem.* 269, 21944-7.
- Belloni, E., Frumkin, A., Scherer, S. W., Rovet, J., Mitchell, H., Barnoski, B., Hing, A., Donis-Keller, H., L.-C., T., and Muenke, M. (1995). Characterization of holoprosencephaly minimal critical region in 7q36. Chromosome 7 workshop 1994. *Cytogenet. Cell. Genet.* 71, 31.
- Belloni, E., Muenke, M., Roessler, E., Traverso, G., Siegel-Bartelt, J., Frumkin, A., Mitchell, H. F., Donis-Keller, H., Helms, C., Hing, A. V., Heng, H. H. G., Koop, B., Martindale, D., Rommens, J. M., Tsui, L.-C., and Scherer, S. W. (1996). Identification of Sonic hedgehog as a candidate gene responsible for holoprosencephaly. *Nat. Genet.* 14, 353-356.

- Berry, R., Wilson, H., Robinson, J., Sandlin, C., Tyson, W., Campbell, J., Porreco, R., and Manchester, D. (1989). Apparent Smith-Lemli-Opitz syndrome and Miller-Dieker syndrome in a family with segregating translocation $t(7;17)(q34;p13.1)$. *Am. J. Med. Genet.* 34, 358-65.
- Bird, A. P. (1986). CpG-rich islands and the function of DNA methylation. *Nature* 321, 209-13.
- Bird, A. P., Taggart, M. H., Nicholls, R. D., and Higgs, D. R. (1987). Non-methylated CpG-rich islands at the human alpha-globin locus: implications for evolution of the alpha-globin pseudogene. *EMBO J.* 6, 999-1004.
- Bogart, M. H., Cunruff, C., Bradshaw, C., Jones, K. L., and Jones, O. W. (1990). Terminal deletions of the long arm of chromosome 7: five new cases. *Am. J. Med. Genet.* 36, 53-5.
- Brock, D. J. H. (1993). *Molecular genetics for the clinician* (Cambridge: University Press).
- Brooks Wilson, A. R., Goodfellow, P. N., Povey, S., Nevanlinna, H. A., de Jong, P. J., and Goodfellow, P. J. (1990). Rapid cloning and characterization of new chromosome 10 DNA markers by Alu element-mediated PCR. *Genomics* 7, 614-20.
- Cawthon, R. M., Weiss, R., Xu, G. F., Viskochil, D., Culver, M., Stevens, J., Robertson, M., Dunn, D., Gesteland, R., O'Connell, P., and et al. (1990). A major segment of the neurofibromatosis type 1 gene: cDNA sequence, genomic structure, and point mutations [published erratum appears in *Cell* 1990 Aug 10;62(3):following 608]. *Cell* 62, 193-201.
- Chasalow, F. I., Blethen, S. L., and Taysi, K. (1985). Possible abnormalities of steroid secretion in children with Smith-Lemli-Opitz syndrome and their parents. *Steroids* 46, 827-43.
- Cherstvoy, E. D., Lazjuk, G. I., Ostrovskaya, T. I., Shved, I. A., Kravtsova, G. I., Lurie, I. W., and Gerasimovich, A. I. (1984). The Smith-Lemli-Opitz syndrome. A detailed pathological study as a clue to a etiological heterogeneity. *Virchows Arch. A. Pathol. Anat. Histopathol.* 404, 413-25.
- Choi, D. W. (1992). Excitotoxic cell death. *J. Neurobiol.* 23, 1261-76.
- Church, D. M., Stotler, C. J., Rutter, J. L., Murrell, J. R., Trofatter, J. A., and Buckler, A. J. (1994). Isolation of genes from complex sources of mammalian genomic DNA using exon amplification. *Nat. Genet.* 6, 98-105.

Church, G. M., and Gilbert, W. (1984). Genomic sequencing. *Proc. Natl. Acad. Sci. U.S.A.* 81, 1991-5.

Clayton, R. B. (1965). Biogenesis of cholesterol and the fundamental steps in terpenoid biosynthesis. In *Q. Rev. Chem. Soc.*, pp. 168-200.

Cremers, F. P., van de Pol, D. J., van Kerkhoff, L. P., Wieringa, B., and Ropers, H. H. (1990). Cloning of a gene that is rearranged in patients with choroideraemia [see comments]. *Nature* 347, 674-7.

Curry, C. J., Carey, J. C., Holland, J. S., Chopra, D., Fineman, R., Golabi, M., Sherman, S., Pagon, R. A., Allanson, J., Shulman, S., and et al. (1987). Smith-Lemli-Opitz syndrome-type II: multiple congenital anomalies with male pseudohermaphroditism and frequent early lethality. *Am. J. Med. Genet.* 26, 45-57.

Dallaire, L., Mitchell, G., Giguere, R., Lefebvre, F., Melancon, S. B., and Lambert, M. (1995). Prenatal diagnosis of Smith-Lemli-Opitz syndrome is possible by measurement of 7-dehydrocholesterol in amniotic fluid. *Prenat. Diagn.* 15, 855-8.

de Die Smulders, C., and Fryns, J. P. (1992). Smith-Lemli-Opitz syndrome: the changing phenotype with age. *Genet. Couns.* 3, 77-82.

Donnai, D., Burn, J., and Hughes, H. (1987). Smith-Lemli-Opitz syndromes: do they include the Pallister-Hall syndrome? *Am. J. Med. Genet.* 28, 741-3.

Duvoisin, R. M., Zhang, C., and Ramonell, K. (1995). A novel metabotropic glutamate receptor expressed in the retina and olfactory bulb. *J. Neurosci.* 15, 3075-83.

Echelard, Y., Epstein, D. J., St Jacques, B., Shen, L., Mohler, J., McMahon, J. A., and McMahon, A. P. (1993). Sonic hedgehog, a member of a family of putative signaling molecules, is implicated in the regulation of CNS polarity. *Cell* 75, 1417-30.

Ericsson, J., Jackson, S. M., and Edwards, P. A. (1996). Synergistic binding of sterol regulatory element-binding protein and NF-Y to the farnesyl diphosphate synthase promoter is critical for sterol-regulated expression of the gene. *J. Biol. Chem.* 271, 24359-64.

Fan, C. M., and Tessier Lavigne, M. (1994). Patterning of mammalian somites by surface ectoderm and notochord: evidence for sclerotome induction by a hedgehog homolog. *Cell* 79, 1175-86.

Fantes, J., Redeker, B., Breen, M., Boyle, S., Brown, J., Fletcher, J., Jones, S., Bickmore, W., Fukushima, Y., Mannens, M., and et al. (1995). Aniridia-associated cytogenetic rearrangements suggest that a position effect may cause the mutant phenotype. *Hum. Mol. Genet.* 4, 415-22.

Foster, J. W., Dominguez Steglich, M. A., Guioli, S., Kowk, G., Weller, P. A., Stevanovic, M., Weissenbach, J., Mansour, S., Young, I. D., Goodfellow, P. N., and et al. (1994). Campomelic dysplasia and autosomal sex reversal caused by mutations in an SRY-related gene. *Nature* 372, 525-30.

Gurrieri, F., Trask, B. J., van den Engh, G., Krauss, C. M., Schinzel, A., Pettenati, M. J., Schindler, D., Dietz Band, J., Vergnaud, G., Scherer, S. W., and et al. (1993). Physical mapping of the holoprosencephaly critical region on chromosome 7q36. *Nat. Genet.* 3, 247-51.

Gyapay, G., Morissette, J., Vignal, A., Dib, C., Fizames, C., Millasseau, P., Marc, S., Bernardi, G., Lathrop, M., and Weissenbach, J. (1994). The 1993-94 Genethon human genetic linkage map [see comments]. *Nat. Genet.* 7, 246-339.

Hayashi, K., and Yandell, D. W. (1993). How sensitive is PCR-SSCP? *Hum. Mutat.* 2, 338-46.

Hayes, K. C., Pronczuk, A., Wood, R. A., and Guy, D. G. (1992). Modulation of infant formula fat profile alters the low-density lipoprotein/high-density lipoprotein ratio and plasma fatty acid distribution relative to those with breast-feeding. *J. Pediatr.* 120, S109-16.

Heckenlively, J. R., Yoser, S. L., Friedman, L. H., and Oversier, J. J. (1988). Clinical findings and common symptoms in retinitis pigmentosa. *Am. J. Ophthalmol.* 105, 504-11.

Hill, S., Creasy, M., and Bunday, S. (1991). A family with three sisters with the 4p- syndrome, originally reported as suffering from the Smith-Lemli-Opitz syndrome. *J. Ment. Defic. Res.* 35, 76-80.

Hobbins, J. C., Jones, O. W., Gottesfeld, S., and Persutte, W. (1994). Transvaginal ultrasonography and transabdominal embryoscopy in the first-trimester diagnosis of Smith-Lemli-Opitz syndrome, type II. *Am. J. Obstet. Gynecol.* 171, 546-9.

Houamed, K. M., Kuijper, J. L., Gilbert, T. L., Haldeman, B. A., O'Hara, P. J., Mulvihill, E. R., Almers, W., and Hagen, F. S. (1991). Cloning, expression, and gene structure of a G protein-coupled glutamate receptor from rat brain. *Science* 252, 1318-21.

Hua, X., Nohturfft, A., Goldstein, J. L., and Brown, M. S. (1996). Sterol resistance in CHO cells traced to point mutation in SREBP cleavage-activating protein. *Cell* 87, 415-426.

Hua, X., Sakai, J., Brown, M. S., and Goldstein, J. L. (1996). Regulated cleavage of sterol regulatory element binding proteins requires sequences on both sides of the endoplasmic reticulum membrane. *J. Biol. Chem.* 271, 10379-84.

Hua, X., Sakai, J., Ho, Y. K., Goldstein, J. L., and Brown, M. S. (1995). Hairpin orientation of sterol regulatory element-binding protein-2 in cell membranes as determined by protease protection. *J. Biol. Chem.* 270, 29422-7.

Hua, X., Wu, J., Goldstein, J. L., Brown, M. S., and Hobbs, H. H. (1995). Structure of the human gene encoding sterol regulatory element binding protein-1 (SREBF1) and localization of SREBF1 and SREBF2 to chromosomes 17p11.2 and 22q13. *Genomics* 25, 667-73.

Hua, X., Yokoyama, C., Wu, J., Briggs, M. R., Brown, M. S., Goldstein, J. L., and Wang, X. (1993). SREBP-2, a second basic-helix-loop-helix-leucine zipper protein that stimulates transcription by binding to a sterol regulatory element. *Proc. Natl. Acad. Sci. U.S.A.* 90, 11603-7.

Hughes, A. E. (1993). Optimization of microsatellite analysis for genetic mapping. *Genomics* 15, 433-4.

Humphries, P. (1993). Hereditary retinopathies: insights into a complex genetic aetiology [editorial; comment]. *Br J Ophthalmol* 77, 469-70.

Irons, M., Elias, E. R., Abuelo, D., Tint, S., and G., S. (1995). Clinical features of the Smith-Lemli-Opitz syndrome and treatment of the cholesterol metabolic defect. *Int. Pediatr.* 10, 28-32.

Irons, M., Elias, E. R., Salen, G., Tint, G. S., and Batta, A. K. (1993). Defective cholesterol biosynthesis in Smith-Lemli-Opitz syndrome [letter]. *Lancet* 341, 1414.

Jeffrey Conn, J., Boss, V., and Chung, D. S. (1994). Second-messenger systems coupled to metabotropic glutamate receptors. In *The metabotropic glutamate receptors*, P. Jeffrey Conn and J. Patel, eds. (Totowa: Humana Press), pp. 59-98.

Jeffreys, A. J., Neumann, R., and Wilson, V. (1990). Repeat unit sequence variation in minisatellites: a novel source of DNA polymorphism for studying variation and mutation by single molecule analysis. *Cell* 60, 473-85.

Johnson, J. A., Aughton, D. J., Comstock, C. H., von Oeyen, P. T., Higgins, J. V., and Schulz, R. (1994). Prenatal diagnosis of Smith-Lemli-Opitz syndrome, type II [see comments]. *Am. J. Med. Genet.* 49, 240-3.

Jordan, S. A., Farrar, G. J., Kenna, P., Humphries, M. M., Sheils, D. M., Kumar Singh, R., Sharp, E. M., Soriano, N., Ayuso, C., Benitez, J., and et al. (1993). Localization of an autosomal dominant retinitis pigmentosa gene to chromosome 7q [comment]. *Nat. Genet.* 4, 54-8.

Joyner, A. L. (1993). Gene Targeting: A Practical Approach. In *The Practical Approach Series*, D. Rickwood and B. D. Hames, eds. (New York: Oxford University Press).

Kelley, R. I., Roessler, E., Hennekam, R. C. M., Feldman, G. L., Kosaki, K., Jones, M. C., Palumbos, J. C., and Muenke, M. (1996). Holoprosencephaly in RSH/Smith-Lemli-Opitz syndrome: Does abnormal cholesterol metabolism affect the function of Sonic hedgehog? *Am. J. Med. Genet.* 66, 478-484.

Knopf, T., Kuhn, R., and Allgeier, H. (1995). Metabotropic glutamate receptors: novel targets for drug development. *Jour. Med. Chem.* 38, 1417-1426.

Kohler, H. G. (1983). Brief clinical report: familial neonatally lethal syndrome of hypoplastic left heart, absent pulmonary lobation, polydactyly, and talipes, probably Smith-Lemli-Opitz (RSH) syndrome. *Am. J. Med. Genet.* 14, 423-8.

Kunz, J., Scherer, S. W., Klawitz, I., Soder, S., Du, Y. Z., Speich, N., Kalff Suske, M., Heng, H. H., Tsui, L. C., and Grzeschik, K. H. (1994). Regional localization of 725 human chromosome 7-specific yeast artificial chromosome clones. *Genomics* 22, 439-48.

Larsen, F., Gundersen, G., Lopez, R., and Prydz, H. (1992). CpG islands as gene markers in the human genome. *Genomics* 13, 1095-107.

Lengauer, C., Green, E. D., and Cremer, T. (1992). Fluorescence in situ hybridization of YAC clones after Alu-PCR amplification. *Genomics* 13, 826-8.

Linton, M. F., R.V., F., and Young, S. G. (1993). Familial hypobetalipoproteinemia. *J. Lipid. Res.* 34, 521-541.

Lovett, M. (1994). Fishing for complements: finding genes by direct selection. *Trends Genet.* 10, 352-7.

Lowry, R. B., Hill, R. H., and Tischler, B. (1983). Survival and spectrum of anomalies in the Meckel syndrome. *Am. J. Med. Genet.* 14, 417-21.

Lowry, R. B., and Yong, S. L. (1980). Borderline normal intelligence in the Smith-Lemli-Opitz (RSH) syndrome. *Am. J. Med. Genet.* 5, 137-43.

Luttrell, L. M., Ostrowski, J., Cotecchia, S., Kendall, H., and Lefkowitz, R. J. (1993). Antagonism of catecholamine receptor signaling by expression of cytoplasmic domains of the receptors. *Science* 259, 1453-7.

MacDermott, A. B., Mayer, M. L., Westbrook, G. L., Smith, S. J., and Barker, J. L. (1986). NMDA-receptor activation increases cytoplasmic calcium concentration in cultured spinal cord neurones [published erratum appears in *Nature* 1986 Jun 26-Jul 2;321(6073):888]. *Nature* 321, 519-22.

Madisen, L., Hoar, D. I., Holroyd, C. D., Crisp, M., and Hodes, M. E. (1987). DNA banking: the effects of storage of blood and isolated DNA on the integrity of DNA. *Am. J. Med. Genet.* 27, 379-90.

Maggio, R., Vogel, Z., and Wess, J. (1993). Reconstitution of functional muscarinic receptors by co-expression of amino- and carboxyl-terminal receptor fragments. *FEBS Lett.* 319, 195-200.

Masu, M., Tanabe, Y., Tsuchida, K., Shigemoto, R., and Nakanishi, S. (1991). Sequence and expression of a metabotropic glutamate receptor. *Nature* 349, 760-5.

McAllister, K. A., Grogg, K. M., Johnson, D. W., Gallione, C. J., Baldwin, M. A., Jackson, C. E., Helmbold, E. A., Markel, D. S., McKinnon, W. C., Murrell, J., and et al. (1994). Endoglin, a TGF-beta binding protein of endothelial cells, is the gene for hereditary haemorrhagic telangiectasia type 1. *Nat. Genet.* 8, 345-51.

McGuire, R. E., Gannon, A. M., Sullivan, L. S., Rodriguez, J. A., and Daiger, S. P. (1995). Evidence for a major gene (RP10) for autosomal dominant retinitis pigmentosa on chromosome 7q: linkage mapping in a second, unrelated family. *Hum. Genet.* 95, 71-4.

McGuire, R. E., Jordan, S. A., Braden, V. V., Bouffard, G. G., Humphries, P., Green, E. D., and Daiger, S. P. (1996). Mapping the RP10 locus for autosomal dominant retinitis pigmentosa on 7q: refined genetic positioning and localization within a well-defined YAC contig. *Genome Res.* 6, 255-266.

McKeever, P. A., and Young, I. D. (1990). Smith-Lemli-Opitz syndrome. II: A disorder of the fetal adrenals? *J. Med. Genet.* 27, 465-6.

Merrer, M. L., Briard, M. L., Girard, S., Mulliez, N., Moraine, C., and Imbert, M. C. (1988). Lethal acro dysgenital dwarfism: a severe lethal condition resembling Smith-Lemli-Opitz syndrome. *J. Med. Genet.* 25, 88-95.

Mills, K., mandel, H., Montemagno, R., Soothill, P., Gershoni-Baruch, R., and Clayton, P. T. (1996). First trimester prenatal diagnosis of Smith-Lemli-Opitz syndrome (7-dehydrocholesterol reductase deficiency). *Pediatr. Res.* 39, 816-819.

Minakami, R., Katsuki, F., and Sugiyama, H. (1993). A variant of metabotropic glutamate receptor subtype 5: an evolutionally conserved insertion with no termination codon. *Biochem. Biophys. Res. Commun.* 194, 622-7.

Monaco, A. P. (1994). Isolation of genes from cloned DNA. *Curr. Opin. Genet. Dev.* 4, 360-5.

Monaco, A. P., Neve, R. L., Colletti Feener, C., Bertelson, C. J., Kurnit, D. M., and Kunkel, L. M. (1986). Isolation of candidate cDNAs for portions of the Duchenne muscular dystrophy gene. *Nature* 323, 646-50.

Monaghan, D. T., Bridges, R. J., and Cotman, C. W. (1989). The excitatory amino acid receptors: their classes, pharmacology, and distinct properties in the function of the central nervous system. *Annu. Rev. Pharmacol. Toxicol.* 29, 365-402.

Murphy, S. N., Thayer, S. A., and Miller, R. J. (1987). The effects of excitatory amino acids on intracellular calcium in single mouse striatal neurons in vitro. *J. Neurosci.* 7, 4145-58.

Nakajima, Y., Iwakabe, H., Akazawa, C., Nawa, H., Shigemoto, R., Mizuno, N., and Nakanishi, S. (1993). Molecular characterization of a novel retinal metabotropic glutamate receptor mGluR6 with a high agonist selectivity for L-2-amino-4-phosphonobutyrate. *J. Biol. Chem.* 268, 11868-73.

Nakanishi, S. (1992). Molecular diversity of glutamate receptors and implications for brain function. *Science* 258, 597-603.

Nakanishi, S. (1994). Metabotropic glutamate receptors: synaptic transmission, modulation, and plasticity. *Neuron* 13, 1031-7.

Natowicz, M. R., and Evans, J. E. (1994). Abnormal bile acids in the Smith-Lemli-Opitz syndrome. *Am. J. Med. Genet.* 50, 364-7.

Ness, G. C. (1994). Developmental regulation of the expression of genes encoding proteins involved in cholesterol homeostasis. *Am. J. Med. Genet.* 50, 355-7.

Niu, L., and Crouse, G. F. (1993). Exon mapping by PCR. *Nucleic Acids Res.* 21, 769-70.

Okamoto, N., Hori, S., Akazawa, C., Hayashi, Y., Shigemoto, R., Mizuno, N., and Nakanishi, S. (1994). Molecular characterization of a new metabotropic glutamate receptor mGluR7 coupled to inhibitory cyclic AMP signal transduction. *J. Biol. Chem.* 269, 1231-6.

Opitz, J. M. (1994). RSH/SLO ("Smith-Lemli-Opitz") syndrome: historical, genetic, and developmental considerations. *Am. J. Med. Genet.* 50, 344-6.

Opitz, J. M., and Lowry, R. B. (1987). Lincoln vs. Douglas again: comments on the papers by Curry et al. Greenberg et al. and Belmont et al. *Am. J. Med. Genet.* 26, 69-71.

Opitz, J. M., Penchaszadeh, V. B., Holt, M. C., Spano, L. M., and Smith, V. L. (1994). Smith-Lemli-Opitz (RSH) syndrome bibliography: 1964-1993. *Am. J. Med. Genet.* 50, 339-43.

Parimoo, S., Kolluri, R., and Weissman, S. M. (1993). cDNA selection from total yeast DNA containing YACs. *Nucleic Acids Res.* 21, 4422-3.

Parimoo, S., Patanjali, S. R., Shukla, H., Chaplin, D. D., and Weissman, S. M. (1991). cDNA selection: efficient PCR approach for the selection of cDNAs encoded in large chromosomal DNA fragments. *Proc. Natl. Acad. Sci. U.S.A.* 88, 9623-7.

Pin, J. P., and Duvoisin, R. (1995). Review: Neurotransmitter receptors I The metabotropic glutamate receptors: structure and functions. *Neuropharm* 34, 1-26.

Pin, J. P., Waeber, C., Prezeau, L., Bockaert, J., and Heinemann, S. F. (1992). Alternative splicing generates metabotropic glutamate receptors inducing different patterns of calcium release in *Xenopus* oocytes. *Proc. Natl. Acad. Sci. U.S.A.* 89, 10331-5.

Pinkel, D., Gray, J. W., Trask, B., van den Engh, G., Fuscoe, J., and van Dekken, H. (1986). Cytogenetic analysis by *in situ* hybridization with fluorescently labeled nucleic acid probes. *Cold Spring Harb. Symp. Quant. Biol.* 1, 151-7.

Porter, J. A., Ekker, S. C., Park, W. J., von Kessler, D. P., Young, K. E., Chen, C. H., Ma, Y., Woods, A. S., Cotter, R. J., Koorin, E. V., and Beachy, P. A. (1996). Hedgehog patterning activity: role of a lipophilic modification mediated by the carboxy-terminal autoprocessing domain. *Cell* 86, 21-34.

Porter, J. A., Young, K. E., and Beachy, P. A. (1996). Cholesterol modification of hedgehog signaling proteins in animal development [see comments]. *Science* 274, 255-9.

Poschl, E., Pollner, R., and Kuhn, K. (1988). The genes for the alpha 1(IV) and alpha 2(IV) chains of human basement membrane collagen type IV are arranged head-to-head and separated by a bidirectional promoter of unique structure. *EMBO J.* 7, 2687-95.

Riddle, R. D., Johnson, R. L., Laufer, E., and Tabin, C. (1993). Sonic hedgehog mediates the polarizing activity of the ZPA. *Cell* 75, 1401-16.

Riley, J., Butler, R., Ogilvie, D., Finniear, R., Jenner, D., Powell, S., Anand, R., Smith, J. C., and Markham, A. F. (1990). A novel, rapid method for the isolation of terminal sequences from yeast artificial chromosome (YAC) clones. *Nucleic Acids Res.* 18, 2887-90.

Roessler, E., Belloni, E., Gaudenz, K., Jay, P., Berta, P., Scherer, S. W., Tsui, L.-C., and Muenke, M. (1996). Mutations in the human Sonic hedgehog gene cause holoprosencephaly. *Nat. Genet.* 14, 357-360.

Rogers, S. W., Andrews, P. I., Gahring, L. C., Whisenand, T., Cauley, K., Crain, B., Hughes, T. E., Heinemann, S. F., and McNamara, J. O. (1994). Autoantibodies to glutamate receptor GluR3 in Rasmussen's encephalitis. *Science* 265, 648-51.

Rommens, J. M., Mar, L., McArthur, J., Tsui, L.-C., and Scherer, S. W. (1994). Towards a transcriptional map of the q21-q22 region of chromosome 7. In *Identification of Transcribed Sequences*, U. Hochgeschwender and K. Gardiner, eds. (New York: Plenum Press), pp. 65-79.

Rothwell, N. V. (1993). *Understanding Genetics; A Molecular Approach* (New York: Wiley-Liss, Inc.).

Rutledge, J. C., Friedman, J. M., Harrod, M. J., Currarino, G., Wright, C. G., Pinckney, L., and Chen, H. (1984). A "new" lethal multiple congenital anomaly syndrome: joint contractures, cerebellar hypoplasia, renal hypoplasia, urogenital anomalies, tongue cysts, shortness of limbs, eye abnormalities, defects of the heart, gallbladder agenesis, and ear malformations. *Am. J. Med. Genet.* 19, 255-64.

Sakai, J., Duncan, E. A., Rawson, R. B., Hua, X., Brown, M. S., and Goldstein, J. L. (1996). Sterol-regulated release of SREBP-2 from cell membranes requires two sequential cleavages, one within a transmembrane segment. *Cell* 85, 1037-46.

Sambrook, J., Fritsch, E. F., and Maniatis, T. (1989). *Molecular Cloning: A Laboratory Manual*, 2nd Edition (New York: Cold Spring Harbor Laboratory Press).

Schafer, A. J., Dominguez Steglich, M. A., Guioli, S., Kwok, C., Weller, P. A., Stevanovic, M., Weissenbach, J., Mansour, S., Young, I. D., Goodfellow, P. N., and et al. (1995). The role of SOX9 in autosomal sex reversal and campomelic dysplasia. *Philos. Trans. R. Soc. Lond. B. Sci.* 350, 271-7; discussion 277-8.

Scherer, S. W., Duvoisin, R. M., Kuhn, R., Heng, H. H. Q., Belloni, E., and Tsui, L.-C. (1996). Localization of two metabotropic glutamate receptor genes, GRM3 and GRM8, to human chromosome 7q. *Genomics* 31, 230-233.

Scherer, S. W., Rommens, J. M., Soder, S., Wong, E., Plavsic, N., Tompkins, B. J., Beattie, A., Kim, J., and Tsui, L. C. (1993). Refined localization and yeast artificial chromosome (YAC) contig-mapping of genes and DNA segments in the 7q21-q32 region. *Hum. Mol. Genet.* 2, 751-60.

Scherer, S. W., Tompkins, B. J., and Tsui, L. C. (1992). A human chromosome 7-specific genomic DNA library in yeast artificial chromosomes. *Mamm. Genome* 3, 179-81.

Scherer, S. W., and Tsui, L.-C. (1991). Cloning and analysis of large DNA molecules. In *Advanced Techniques in Chromosome Research*, K. Adolph, ed. (New York: Marcel Dekkar), pp. 33-72.

Schwartz, S., Meekins, J., Panny, S. R., Sun, C. C., and Cohen, M. M. (1983). Brief clinical report: cebocephaly-holoprosencephaly in a newborn girl with a terminal 7q deletion [46,XX,del(7)(pter leads to q32:)]. *Am. J. Med. Genet.* 15, 141-4.

Shiang, R., Thompson, L. M., Zhu, Y. Z., Church, D. M., Fielder, T. J., Bocian, M., Winokur, S. T., and Wasmuth, J. J. (1994). Mutations in the transmembrane domain of FGFR3 cause the most common genetic form of dwarfism, achondroplasia. *Cell* 78, 335-42.

Sladeczek, F., Pin, J. P., Recasens, M., Bockaert, J., and Weiss, S. (1985). Glutamate stimulates inositol phosphate formation in striatal neurones. *Nature* 317, 717-9.

Smith, D. W., Lemli, L., and Opitz, J. M. (1964). A newly recognized syndrome of multiple congenital anomalies. *Jour. Pediatr.* 64, 210-217.

Stapleton, P., Weith, A., Urbanek, P., Kozmik, Z., and Busslinger, M. (1993). Chromosomal localization of seven PAX genes and cloning of a novel family member, PAX-9. *Nat. Genet.* 3, 292-8.

Steinberg, D., and Avigan, J. (1960). Studies of cholesterol biosynthesis II. The role of desmosterol in the biosynthesis of cholesterol. In *J. Biol. Chem.* pp. 3127-3129.

- Stuart, E. T., and Gruss, P. (1995). PAX genes: what's new in developmental biology and cancer? *Hum. Mol. Genet.* 1717-20.
- Sudzak, P. D., Thomsen, C., Mulvihill, E., and Kristensen, P. (1994). Molecular cloning, expression, and characterization of metabotropic glutamate receptor subtypes. In *The Metabotropic Glutamate Receptors*, P. Jeffrey Conn and J. Patel, eds. (Totowa: Humana Press), pp. 1-30.
- Sugiyama, H., Ito, I., and Hirono, C. (1987). A new type of glutamate receptor linked to inositol phospholipid metabolism. *Nature* 325, 531-3.
- Tagle, D. A., and Collins, F. S. (1992). An optimized Alu-PCR primer pair for human-specific amplification of YACs and somatic cell hybrids. *Hum. Mol. Genet.* 1, 121-2.
- Tamura, T., Izumikawa, Y., Kishino, T., Soejima, H., Jinno, Y., and Niikawa, N. (1994). Assignment of the human PAX4 gene to chromosome band 7q32 by fluorescence in situ hybridization. *Cytogenet. Cell. Genet.* 66, 132-4.
- Tanabe, Y., Masu, M., Ishii, T., Shigemoto, R., and Nakanishi, S. (1992). A family of metabotropic glutamate receptors. *Neuron* 8, 169-79.
- Thomas, R. J. (1995). Excitatory amino acids in health and disease. *J. Am. Geriatr. Soc.* 43, 1279-89.
- Tint, G. S., Irons, M., Elias, E. R., Batta, A. K., Frieden, R., Chen, T. S., and Salen, G. (1994). Defective cholesterol biosynthesis associated with the Smith-Lemli-Opitz syndrome [see comments]. *N. Engl. J. Med.* 330, 107-13.
- Vallett, S. M., Sanchez, H. B., Rosenfeld, J. M., and Osborne, T. F. (1996). A direct role for sterol regulatory element binding protein in activation of 3-hydroxy-3-methylglutaryl coenzyme A reductase gene. *J. Biol. Chem.* 271, 12247-53.
- Wallace, M., Zori, R. T., Alley, T., Whidden, E., Gray, B. A., and Williams, C. A. (1994). Smith-Lemli-Opitz syndrome in a female with a de novo, balanced translocation involving 7q32: probable disruption of an SLOS gene. *Am. J. Med. Genet.* 50, 368-74.
- Wallace, M. R., Marchuk, D. A., Andersen, L. B., Letcher, R., Odeh, H. M., Saulino, A. M., Fountain, J. W., Brereton, A., Nicholson, J., Mitchell, A. L., and et al. (1990). Type 1 neurofibromatosis gene: identification of a large transcript disrupted in three NF1 patients [published erratum appears in *Science* 1990 Dec 21;250(4988):1749]. *Science* 249, 181-6.

Wang, X., Briggs, M. R., Hua, X., Yokoyama, C., Goldstein, J. L., and Brown, M. S. (1993). Nuclear protein that binds sterol regulatory element of low density lipoprotein receptor promoter. II. Purification and characterization. *J. Biol. Chem.* 268, 14497-504.

Weber, J. L., and May, P. E. (1989). Abundant class of human DNA polymorphisms which can be typed using the polymerase chain reaction. *Am J Hum. Genet* 44, 388-96.

White, M. B., Carvalho, M., Derse, D., O'Brien, S. J., and Dean, M. (1992). Detecting single base substitutions as heteroduplex polymorphisms. *Genomics* 12, 301-6.

Wunderle, V. M., Ramkissoon, Y. D., Kwok, C., Korn, R. M., King, V. E., and Goodfellow, P. N. (1994). Breakpoint break for consortium studying adult polycystic kidney disease. *Cell* 77, 785-6.

Yang, S. P., Saxon, P. J., Wertz, A. W., Bachman, R. P., Kelley, R. I., Boser, A. B., Shaffer, L. G., Lindsay, E. A., and Patel, P. I. (1994). Biochemical and molecular dissection of the Smith-Lemli-Opitz type II phenotype. In *Proceedings of the David Smith Workshop on Malformations and Morphogenesis*, Montreal, pp. 32.

Yokoyama, C., Wang, X., Briggs, M. R., Admon, A., Wu, J., Hua, X., Goldstein, J. L., and Brown, M. S. (1993). SREBP-1, a basic-helix-loop-helix-leucine zipper protein that controls transcription of the low density lipoprotein receptor gene. *Cell* 75, 187-97.

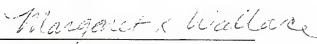
Young, R. S., Weaver, D. D., Kukulich, M. K., Heerema, N. A., Palmer, C. G., Kawira, E. L., and Bender, H. A. (1984). Terminal and interstitial deletions of the long arm of chromosome 7: a review with five new cases. *Am. J. Med. Genet* 17, 437-50.

Yunis, J. J. (1976). High resolution of human chromosomes. *Science* 191, 1268-70.

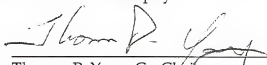
BIOGRAPHICAL SKETCH

Tiffany L. Alley was born in Miami, Florida, on June 16, 1970. She attended Cooper City High School in Cooper City, Florida, and began her undergraduate education at the University of Florida in the Summer of 1988. On May 2, 1992, she received her Bachelor of Science in microbiology. Tiffany continued her education at the University of Florida and began her doctoral studies under the guidance of Dr. Margaret R. Wallace in the Department of Biochemistry and Molecular Biology in 1992. She earned her Doctor of Philosophy degree in May, 1997 in biochemistry and molecular biology.

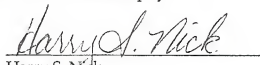
I certify that I have read this study and that in my opinion it conforms to acceptable standards of scholarly presentation and is fully adequate, in scope and quality, as a dissertation for the degree of Doctor of Philosophy.


Margaret R. Wallace, Chair
Associate Professor of Biochemistry
and Molecular Biology

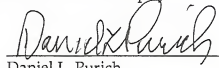
I certify that I have read this study and that in my opinion it conforms to acceptable standards of scholarly presentation and is fully adequate, in scope and quality, as a dissertation for the degree of Doctor of Philosophy.


Thomas P. Yang, Co-Chair
Associate Professor of Biochemistry
and Molecular Biology

I certify that I have read this study and that in my opinion it conforms to acceptable standards of scholarly presentation and is fully adequate, in scope and quality, as a dissertation for the degree of Doctor of Philosophy.


Harry S. Nick
Associate Professor of Biochemistry
and Molecular Biology

I certify that I have read this study and that in my opinion it conforms to acceptable standards of scholarly presentation and is fully adequate, in scope and quality, as a dissertation for the degree of Doctor of Philosophy.

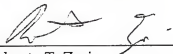

Daniel L. Purich
Professor of Biochemistry and
Molecular Biology

I certify that I have read this study and that in my opinion it conforms to acceptable standards of scholarly presentation and is fully adequate, in scope and quality, as a dissertation for the degree of Doctor of Philosophy.



Charles M. Allen
Professor of Biochemistry and
Molecular Biology

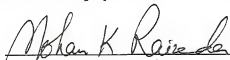
I certify that I have read this study and that in my opinion it conforms to acceptable standards of scholarly presentation and is fully adequate, in scope and quality, as a dissertation for the degree of Doctor of Philosophy.



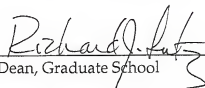
Roberto T. Zori
Assistant Professor of Pathology
and Laboratory Medicine

This dissertation was submitted to the Graduate Faculty of the College of Medicine and to the Graduate School and was accepted as partial fulfillment of the requirements for the degree of Doctor of Philosophy.

May 1997



Nolan K. Reinhardt
Dean, College of Medicine



Richard J. Felt
Dean, Graduate School